Molecular functions of the transcription factors E2A and E2-2 in controlling germinal center B cell and plasma cell development

Miriam Wöhner, Hiromi Tagoh,* Ivan Bilic,* Markus Jaritz, Daniela Kostanova Poliakova, Maria Fischer, and Meinrad Busslinger

Research Institute of Molecular Pathology, Vienna Biocenter, A-1030 Vienna, Austria

E2A is an essential regulator of early B cell development. Here, we have demonstrated that E2A together with E2-2 controlled germinal center (GC) B cell and plasma cell development. As shown by the identification of regulated E2A,E2-2 target genes in activated B cells, these E-proteins directly activated genes with important functions in GC B cells and plasma cells by inducing and maintaining DNase I hypersensitive sites. Through binding to multiple enhancers in the *Igh* 3′ regulatory region and *Aicda* locus, E-proteins regulated class switch recombination by inducing both *Igh* germline transcription and AID expression. By regulating 3′ *Igk* and *Igh* enhancers and a distal element at the *Prdm1* (Blimp1) locus, E-proteins contributed to *Igk*, *Igh*, and *Prdm1* activation in plasmablasts. Together, these data identified E2A and E2-2 as central regulators of B cell immunity.

The Journal of Experimental Medicine

B cell immunity provides acute and long-term protection of the host against infections through the generation and secretion of high-affinity antibodies that recognize a shear unlimited number of pathogens. This enormous adaptive potential of B cells is brought about by V(D)J recombination of the immunoglobulin heavy chain (*Igh*) and light chain (*Igk* and *Igl*) genes in early B cell development, and by subsequent affinity maturation of the Ig heavy chain in late B cell differentiation (Victora and Nussenzweig, 2012). Somatic hypermutation alters the antigen-binding V_H sequences of the Ig heavy-chain, whereas class switch recombination (CSR) exchanges the C_H exons to generate Ig isotypes with distinct effector functions (Chaudhuri and Alt, 2004). Whereas the activation-induced deaminase (AID) is an essential regulator of both processes (Muramatsu et al., 2000), somatic hypermutation only takes place in germinal centers (GCs), which are formed upon antigen exposure by the interplay of T follicular helper (Tfh) cells and follicular (FO) B cells in secondary lymphoid organs (Victora and Nussenzweig, 2012). Affinity-based selection in this specialized compartment leads to clonal expansion of B cells expressing high-affinity B cell receptors, which subsequently differentiate to proliferating, antibody-secreting plasmablasts (Victora and Nussenzweig, 2012). Upon migration to specialized bone marrow niches, plasmablasts differentiate into long-lived quiescent plasma cells secreting high amounts of antibodies (Nutt et al., 2015). While many transcription factors are involved in coordinating these B cell responses, we have here studied the role of E-proteins in the regulation of these processes.

Basic helix–loop–helix (bHLH) transcription factors can be subdivided into different classes based on biochemical and functional properties (Murre, 2005). Class I bHLH proteins, also known as E-proteins, consist of the three members, E2A (*Tcf3*), E2-2 (*Tcf4*), and HEB (*Tcf12*; Murre, 2005), which bind the E-box (CANNTG) motif with similar sequence specificity (Fig. S1 A). E-proteins are broadly expressed and heterodimerize with class II bHLH proteins in nonlymphoid cell types. Within the lymphoid system, E-proteins function as homodimers or heterodimers with a different E-protein (Bain et al., 1993; Shen and Kadesch, 1995). E-proteins are thought to mainly function as transcriptional activators, as they interact with the co-activators p300 and CBP (Bradney et al., 2003; Bayly et al., 2004), as well as the promoter recognition factor TFIID (Chen et al., 2013). The activity of E-proteins is controlled by the inhibitor of DNA binding proteins, which are HLH proteins lacking the basic DNA-binding domain, and are thus capable of sequestering E-proteins into DNA-binding–incompetent heterodimers (Kee, 2009).

E-proteins control different aspects of B cell development (Murre, 2005). E2A is required for the commitment of lymphoid progenitors to the B cell lineage (Bain et al.,

*H. Tagoh and I. Bilic contributed equally to this paper.

Correspondence to Meinrad Busslinger: busslinger@imp.ac.at

I. Bilic's present address is Baxalta Innovations GmbH, A-1221 Vienna, Austria.

Abbreviations used: 3C, chromosome conformation capture; 3D, three dimensional; AID, activation-induced deaminase; ASC, antibody-secreting cell; ATAC, assay for transposase-accessible chromatin; bHLH, basic helix–loop–helix; ChIP, chromatin immunoprecipitation; CSR, class switch recombination; DHS, DNase I hypersensitive; DKO, double KO; ELISPOT, enzyme-linked immunospot; FO, follicular; GC, germinal center; GLT, germline transcript; Lin, lineage; MZ, marginal zone; NP-KLH, 4-hydroxy-3-nitrophenylacetyl-conjugated keyhole limpet hemocyanin; RPKM, reads per kilobase of exon per million mapped sequence reads; RPM, reads per gene per million mapped sequence reads; RR, regulatory region; SRBC, sheep RBC; Tfh, T follicular helper.

© 2016 Wöhner et al. This article is distributed under the terms of an Attribution–Noncommercial–Share Alike–No Mirror Sites license for the first six months after the publication date (see http://www.rupress.org/terms). After six months it is available under a Creative Commons License (Attribution–Noncommercial–Share Alike 3.0 Unported license, as described at http://creativecommons.org/licenses/by-nc-sa/3.0/).

The Rockefeller University Press $30.00
J. Exp. Med. 2016 Vol. 213 No. 7 1201–1221
www.jem.org/cgi/doi/10.1084/jem.20152002

1994; Zhuang et al., 1994). E2A is also essential for V_κ-J_κ recombination (Inlay et al., 2004) and early B cell development (Kwon et al., 2008). Inactivation of all E-proteins in activated B cells by overexpression of the antagonist ID3 revealed an important role for these transcription factors in promoting CSR to different IgG isotypes (Quong et al., 1999) and activating the *Aicda* (AID) gene (Sayegh et al., 2003). As shown by conditional *Tcf3* inactivation, E2A is largely dispensable for the formation and function of different mature B cell types and plasma cells, except for GC B cell differentiation, which is reduced but not lost in the absence of E2A (Kwon et al., 2008). It is, however, possible that the activity of another E-protein may compensate for the loss of E2A in late B cell differentiation in analogy to the cooperative function of E2A and HEB in T cell development (Jones-Mason et al., 2012).

Here, we have used conditional mutagenesis to demonstrate a cooperative role of E2A and E2-2 in controlling GC B cell and plasma cell development. Using genome-wide approaches, we comprehensively analyzed the molecular role of E2A and E2-2 in late B cell development, which revealed that these E-proteins directly control many essential functions of GC B cells and plasma cells. Hence, these experiments identified E2A and E2-2 as central regulators of B cell immunity.

RESULTS

Efficient generation of mature B cells upon combined loss of E2A and E2-2

As shown by RNA-seq, *Tcf3* (E2A) was highly expressed in FO and GC B cells compared with *Tcf4* (E2-2) and *Tcf12* (HEB; Fig. 1 A). *Tcf4* was, however, similarly expressed like *Tcf3* in bone marrow plasma cells in contrast to *Tcf12*. We therefore hypothesized that *Tcf4* likely compensates for the loss of E2A in late B cell development. To test this hypothesis, we used the *Cd23*-Cre line, which initiates Cre-mediated deletion in immature B cells of the spleen (Kwon et al., 2008), the floxed *Tcf3* allele (*Tcf3^{fl}*), which expresses a nonfunctional E2A-GFP fusion protein upon Cre-mediated elimination of the bHLH domain-encoding exons (Kwon et al., 2008), and the *Tcf4^{fl}* allele (Bergqvist et al., 2000). We thus generated *Tcf3$^{fl/fl}$ Tcf4$^{fl/fl}$* mice (referred to as *Tcf3,4$^{fl/fl}$* or 'WT' mice) and *Cd23*-Cre *Tcf3$^{fl/fl}$ Tcf4$^{fl/fl}$* mice (referred to as *Cd23*-Cre *Tcf3,4$^{fl/fl}$* for the mice and DKO for the respective B cells). As shown by flow cytometric analysis, mature B cells ($B220^+CD19^+IgM^{lo}IgD^{hi}$), FO B cells ($B220^+CD19^+CD21^{int}CD23^{hi}$), and marginal zone (MZ) B cells ($B220^+CD19^+CD21^{hi}CD23^{lo/-}$) were present at similar or slightly reduced numbers in the spleen of *Cd23*-Cre *Tcf3,4$^{fl/fl}$* mice compared with *Tcf3,4$^{fl/fl}$* littermates (Fig. 1 B). GFP expression furthermore suggested complete *Tcf3* deletion in FO and MZ B cells of *Cd23*-Cre *Tcf3,4$^{fl/fl}$* mice (Fig. 1 B), which was confirmed by PCR genotyping and immunoblot analysis with an E2A antibody (Fig. 1, C and D). In contrast, *Tcf3* and *Tcf4* were only partially deleted in splenic and peritoneal B-1 cells ($B220^{lo}CD19^+$) of the *Cd23*-Cre *Tcf3,4$^{fl/fl}$* genotype (Fig. 1 C and not depicted). Hence, FO and MZ B cells were efficiently generated in the absence of E2A and E2-2.

Loss of GC B cell differentiation in the absence of E2A and E2-2

To study the role of E2A and E2-2 in GC B cell development, we immunized mice with 4-hydroxy-3-nitrophenylacetyl-conjugated keyhole limpet hemocyanin (NP-KLH). 7 d after immunization, GC B cells could be detected in the spleen of *Cd23*-Cre *Tcf4$^{fl/fl}$* and control *Tcf3,4$^{fl/fl}$* mice as $Fas^+GL7^+CD19^+B220^+$ cells by flow cytometry (Fig. 2 A) and as $GL7^+$ cells on histological sections (Fig. 2 B). As previously shown (Kwon et al., 2008), the GC B cell number and GC size were strongly reduced in *Cd23*-Cre *Tcf3$^{fl/fl}$* mice (Fig. 2, A and B), consistent with a prominent role of E2A in GC B cell development. GC B cells were, however, completely absent in *Cd23*-Cre *Tcf3,4$^{fl/fl}$* mice (Fig. 2, A and B). These observations were confirmed by analyzing splenic GC B cells at day 14 and lymph node GC B cells at day 7 after NP-KLH immunization (Fig. 2, C and D), as well as by investigating splenic GC B cells at day 14 after immunization with sheep RBCs (SRBCs; Fig. 2 E). Hence, the development of GC B cells critically depends on both E2A and E2-2.

Gene regulation by E2A and E2-2 in anti-CD40 and IL-4–activated B cells

We next determined the E2A,E2-2–dependent gene expression program in activated B cells that were stimulated with anti-CD40 antibodies and IL-4, which mimics the T cell help required for GC B cell differentiation. First, we determined the genome-wide pattern of E-protein binding by chromatin immunoprecipitation (ChIP)-seq of unstimulated FO B cells and activated B cells after stimulation with anti-CD40 and IL-4 for 2 d. ChIP was performed with an E2A antibody after cross-linking of the chromatin with formaldehyde alone (single cross-linking [s]) or with a combination of disuccinimidyl glutarate and formaldehyde (double cross-linking [d]). E2A binding at the *Pou2af1* and *Mef2b* loci (Fig. 3 A) and genome-wide E2A peak calling (Fig. S1, B and C) revealed a significant overlap of the peaks identified with both cross-linking methods. We therefore called an E2A peak only if it was detected by both single and double cross-linking in the same cell type. Based on this stringent peak calling, we determined 5,314 and 7,571 E2A peaks in FO (day 0) and activated B cells (day 2), respectively, which contained the consensus E2A-binding motif (Figs. 3 B and S1, D and E). Peak-to-gene assignment defined 3,893 and 4,946 E2A-bound target genes in FO and activated B cells, respectively (Fig. 3 B).

Second, we determined the transcriptome of FO B cells of the *Tcf3,4$^{fl/fl}$* (WT) and *Cd23*-Cre *Tcf3,4$^{fl/fl}$* (DKO) genotypes before or after anti-CD40 and IL-4 stimulation for 1, 2, or 3 d by RNA-seq. Gene expression comparison of activated WT and DKO B cells at day 3 identified 157 activated and 108 repressed genes, which were selected for an expression difference of greater than threefold, an adjusted p-value of <0.05, and an RPKM value of >3 in stimulated WT (activated) or DKO (repressed) B cells, respectively (Fig. S1 F).

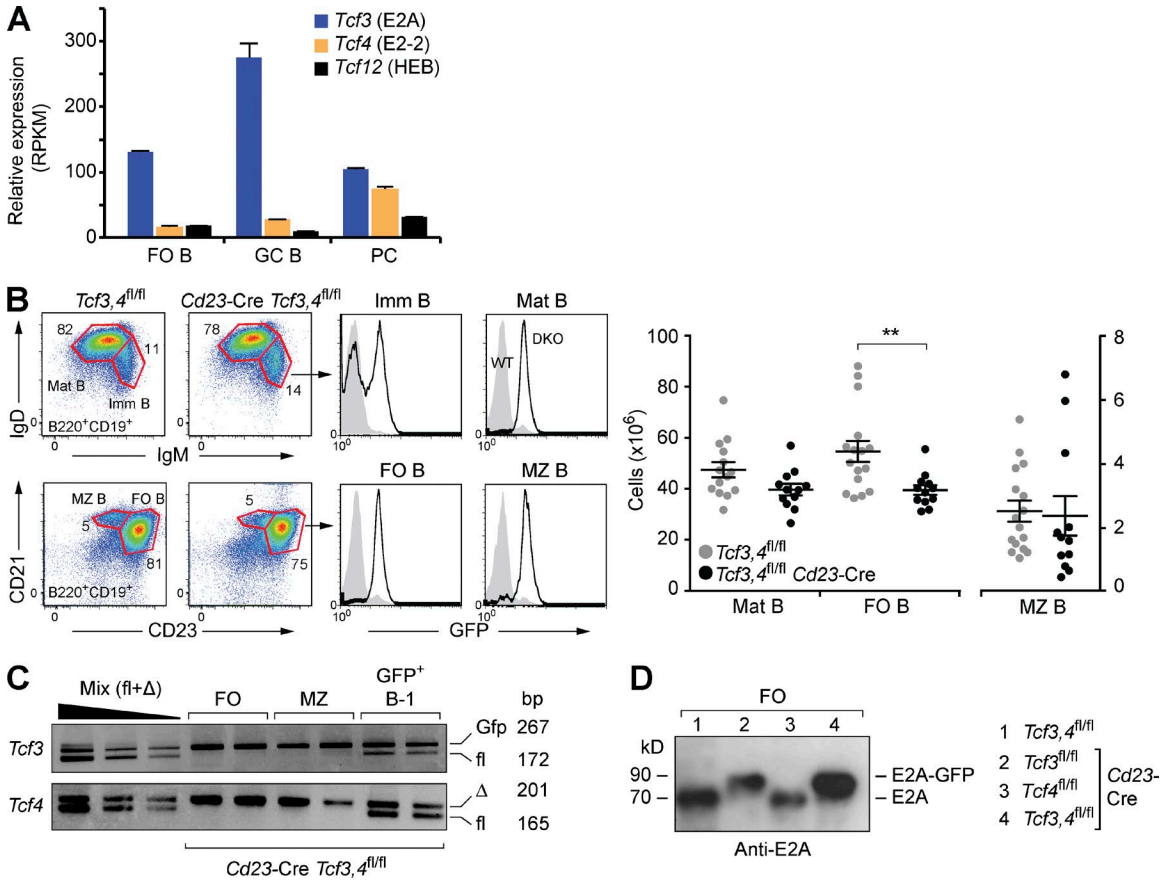

Figure 1. **Efficient generation of mature B cells in the absence of E2A and E2-2.** (A) Expression of *Tcf3*, *Tcf4*, and *Tcf12* in lymph node FO B cells, splenic GC B cells, and bone marrow plasma cells (PC) of WT mice is shown as normalized gene expression value (RPKM) with SEM, based on two RNA-seq experiments for each cell type. (B) Flow cytometric analysis of splenic B cells from mice of the indicated genotypes at the age of 8–12 wk. Numbers refer to the percentage of cells in the indicated gate. GFP expression is shown for immature (Imm), mature (Mat), MZ, and FO B cells of the DKO (black line) and WT (gray surface) genotypes. To the right, absolute numbers of the indicated cell types are shown with SEM. **, $P < 0.01$, (Student's *t* test). Each symbol represents one mouse, and the data are pooled from five independent experiments. (C) PCR detection of *Tcf3* and *Tcf4* deletion in sorted FO B, MZ B, and GFP$^+$ B-1a cells from the spleen of two DKO mice. The positions of the PCR fragments (size shown in base pairs) corresponding to the deleted *Tcf3* (Gfp), deleted *Tcf4* (Δ) and intact floxed (fl) alleles are indicated. Mix (fl+Δ) refers to a 1:1 mixture of sorted *Tcf3,4*$^{fl/fl}$ and *Cd23*-Cre *Tcf3,4*$^{fl/fl}$ FO B cells. (D) Immunoblot analysis of E2A and E2A-GFP proteins (size shown in kilodaltons) in CD43$^-$ FO B cells from lymph nodes of the indicated genotypes.

By determining the overlap between the E2A-bound genes (Fig. 3 B) and E2A,E2-2-regulated genes (Fig. S1 F), we identified 120 potentially directly activated and 32 potentially directly repressed E2A,E2-2 target genes (Fig. 3 C and Table S1). Notably, the vast majority (76.4%) of all activated genes (157) were also bound by E2A, in contrast to only 29.6% of all repressed genes (108; Fig. 3 C). Hence, E2A and E2-2 primarily activate gene transcription, whereas they repress genes mainly in an indirect manner in activated B cells.

More than half of all activated E-protein target genes code for cell surface receptors (20), signal transducers (26), and transcriptional regulators (22), which suggests a role for E2A and E2-2 in B cell signaling (Fig. 3 D). Importantly, four activated target genes (*Icosl*, *Mef2b*, *Pou2af1*, and *Neil1*) are known to play important roles in GC B cell differentiation (Fig. 3 E). E2A and E2-2 also activated three transcription factor genes (*Prdm1* [Blimp1], *Xbp1*, and *Eaf2*) with important functions in plasma cell differentiation (Fig. 3 F), as well as four genes (*Mzb1*, *Edem1*, *Fcrla*, and *Wfs1*) that contribute to the homeostatic control of the ER (Fig. S2 A). The E2A,E2-2–dependent regulation of additional transcription factor genes with known functions in B cells (*Bhlhe41*, *Id3*, *Bhlha15*, *Klf2*, *Arid3a*, and *Bcl3*) and T cells (*Aire*, *Ahr*, *Bcl6b*, and *Hivep3*) are shown in Fig. S2 B. Another functional class of eight activated target genes codes for potentially inhibitory (Sit1, Lax1, Rasal1, Ptpn3, and Dusp6) or stimulatory (Lat, Src, and Ralgds) signal transducers of BCR signaling (Figs. 3 G and S2 C). Finally, we identified 23 activated target genes coding for cell surface proteins, signal transducers, and cytoskeletal proteins involved in cell adhesion and migration (Figs. 3 H and S2 D), indicating that E2A and E2-2 may control the migratory or sessile behavior of activated B cells.

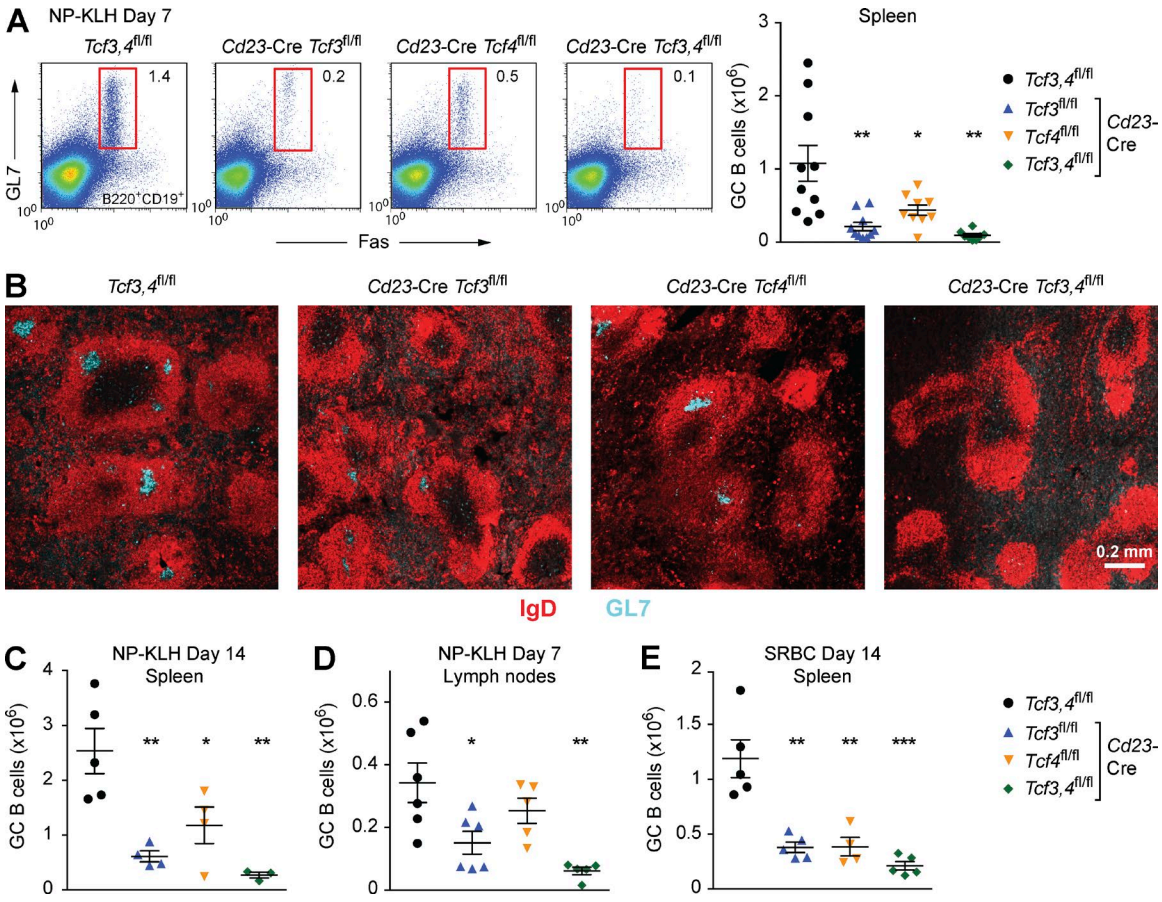

Figure 2. **Loss of GC B cell development in the absence of E2A and E2-2.** (A) Splenic GC B cells of the indicated genotypes were analyzed by flow cytometry at day 7 after immunization with NP-KLH. Absolute numbers of GC B cells in the spleen of the different genotypes are shown with SEM (right). *, $P < 0.05$; **, $P < 0.01$; ***, $P < 0.001$, (Student's *t* test) calculated relative to the *Tcf3,4*$^{fl/fl}$ genotype (left). Each symbol represents one mouse, and the data are pooled from two experiments. (B) Histological analysis of GCs at day 7 after NP-KLH immunization. Cryosections of the spleen were stained with anti-GL7 (blue) and anti-IgD (red) antibodies. (C–E) GC B cell numbers in the spleen (C) and lymph nodes (D) of the indicated genotypes at day 14 or 7 after NP-KLH immunization, respectively, and in the spleen (E) at day 14 after sheep red blood cell (SRBC) immunization. Statistical analysis was performed as described in A. The data are from one experiment representative of three experiments (C) or are pooled from two experiments (D and E).

E-proteins induce and maintain open chromatin at activated target genes

To investigate a possible role of E-proteins in controlling regulatory elements at activated target genes, we mapped open chromatin regions (known as DNase I hypersensitive [DHS] sites) by assay for transposase-accessible chromatin (ATAC)-seq (Buenrostro et al., 2013) in activated WT and DKO B cells at day 2 of anti-CD40 and IL-4 stimulation. The chromatin accessibility, which was measured as read density of each DHS site, was increased at E2A peaks of activated genes in WT B cells compared with DKO B cells (Fig. 4 A, left). In contrast, the densities of DHS sites lacking E2A binding at activated genes were similar to those of all DHS sites in both cell types (Fig. 4 A, right). This suggests that E-proteins are essential for inducing or maintaining DHS sites at activated target genes. As exemplified for the *Lmo7* gene, the induction of a DHS site correlated with increased E2A binding upon stimulation of WT B cells, but not of DKO B cells (Fig. 4 B). Conversely, an E2A-bound DHS site, which was detected at the *Selplg* gene in FO and activated B cells, was specifically lost in activated DKO B cells (Fig. 4 B). We conclude therefore that E-proteins are required for the induction and maintenance of DHS sites at activated target genes.

E2A and E2-2 control CSR by regulating *Igh* transcription

We next investigated CSR to IgG1 in GC B cells (Fas^+GL7^+), which were still formed in Peyer's patches in the absence of E2A and E2-2 (Fig. 5 A). $IgG1^+Fas^+$ GC B cells were absent in Peyer's patches of *Cd23*-Cre *Tcf3,4*$^{fl/fl}$ mice (Fig. 5 A). Moreover, $IgG1^+Fas^+$ B cells were more strongly reduced in *Cd23*-Cre *Tcf3*$^{fl/fl}$ mice compared with *Cd23*-Cre *Tcf4*$^{fl/fl}$ mice, indicating that E2A is the dominant E-protein controlling IgG1 CSR in Peyer's patches (Fig. 5 A). A similar situation was observed upon in vitro stimulation of FO B cells

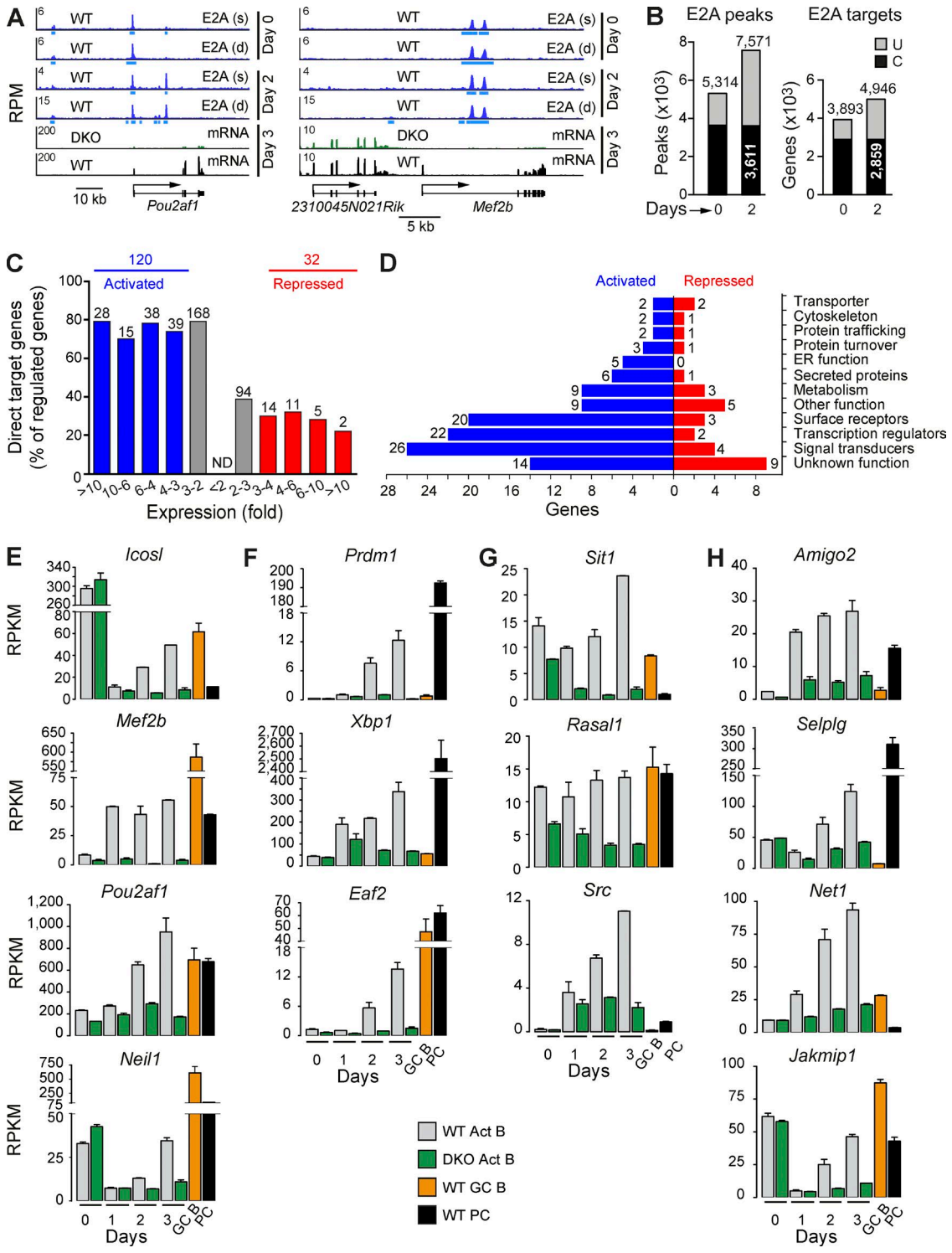

Figure 3. **Gene expression changes in the absence of E2A and E2-2 in anti-CD40 and IL-4–stimulated B cells.** (A) RNA- and ChIP-seq analysis of the activated target genes *Pou2af1* and *Mef2b*. CD43⁻ B cells from lymph nodes of WT and DKO mice were stimulated with anti-CD40 and IL-4 for up to 3 d before RNA-seq analysis. For ChIP-seq, unstimulated (day 0) and stimulated (day 2) WT B cells were single (s) or double (d) cross-linked followed by ChIP with an E2A antibody. E2A peaks and mRNA signals are shown together with the exon–intron structure of the indicated genes and a scale bar (in kilobases). Bars below the ChIP-seq track indicate E2A-binding regions identified by MACS peak calling. (B) Identification of E2A peaks and bound target genes in unstimulated (day 0) and stimulated (day 2) B cells, as described in Fig. S1 (B and C) and defined by peak-to-gene assignment, respectively. Common (C, black) and unique (U, gray) peaks and target genes are shown for both B cell types. (C) Activated and repressed E2A,E2-2 target genes in stimulated B cells.

from WT and mutant lymph nodes for 4 d with anti-CD40 and IL-4 (Fig. 5 B). CSR to IgG1 was lost in DKO B cells, although the proliferation of these cells was only minimally reduced compared with WT B cells, as shown by dilution of the CellTrace Violet reagent (Fig. 5 C). Notably, treatment of FO B cells with LPS and IL-4 for 4 d revealed an equally important role of E2A and E2-2 in controlling CSR to IgG1 (Fig. 5 D) in contrast to the dominant role of E2A observed upon anti-CD40 plus IL-4 stimulation (Fig. 5 B). Hence, both E2A and E2-2 are essential for IgG1 CSR.

The switch regions of *Igh* constant genes are made accessible for CSR by germline transcription from an upstream I promoter that is activated upon signaling by specific cytokines (Chaudhuri and Alt, 2004). Stimulation of WT B cells with anti-CD40 and IL-4 for 3 d strongly induced the expression of Iγ1 and Iε germline transcripts (GLTs) in addition to the constitutively expressed Iμ transcript (Fig. 5 E). Importantly, the Iμ and Iε GLTs were 2.3- and 7-fold reduced in activated DKO B cells (Fig. 5 E). Unexpectedly, the Iγ1 GLT was only minimally decreased upon loss of E2A and E2-2, indicating that the absence of IgG1 CSR in DKO B cells is caused by another defect (Fig. 5 E). E2A binding was detected at the Iγ1 promoter and a downstream enhancer (Fig. 5 F), as well as at the Iε promoter (Fig. 5 G) in activated B cells. At both genes, DHS sites remained unaffected, and active (H3K27ac) chromatin was minimally reduced in activated DKO B cells, suggesting that the decrease of Iε GLTs is caused by a defect at a distant regulatory element. Indeed, the abundance of H3K27ac was strongly reduced, and the DHS sites were lost at three enhancers (HS3A, HS1,2, and HS3B) of the *Igh* 3′ regulatory region (3′RR) in activated DKO B cells (Fig. 5 H). Notably, E2A binding was observed at all three enhancers (Fig. 5 H). As the 3′RR is important for CSR to all Igh isotypes (Vincent-Fabert et al., 2010; Saintamand et al., 2015), we conclude that E2A and E2-2 regulate *Igh* germline transcription, and thus CSR, by controlling the activity of the 3′RR.

E-proteins regulate the *Aicda* locus by binding to multiple enhancers

Retroviral overexpression of the antagonist ID3 in activated B cells demonstrated a role for E-proteins in controlling *Aicda* expression (Sayegh et al., 2003). We confirmed this finding by providing genetic evidence that the loss of E2A and E2-2 prevented *Aicda* activation in response to anti-CD40 and IL-4 stimulation (Fig. 6 A). The *Aicda* locus contains five enhancer regions (E1-E5), which interact with each other and the promoter (P1) to activate *Aicda* expression (Kieffer-Kwon et al., 2013). We detected E2A binding not only at the previously identified site in the intronic enhancer E4 (Sayegh et al., 2003), but also at the upstream enhancers E1 and E2 and downstream enhancer E5 in activated B cells at day 2 of anti-CD40 and IL-4 treatment (Fig. 6 B). Active chromatin (H3K27ac) was strongly reduced at all E2A-bound enhancers (E1, E2, E4, and E5) in activated DKO B cells relative to WT B cells, but the abundance of H3K27ac was similar in both cell types at the enhancer E3 (Fig. 6 B) and in a genomic control region (Fig. S1 G). The density of the DHS sites at all four E2A-bound enhancers was also decreased in activated DKO B cells (Fig. 6 B). Collectively, these data indicate that E-proteins activate *Aicda* transcription by controlling multiple enhancers.

As E-proteins affect CSR by regulating *Aicda* and *Igh* GLTs, we discriminated between these two functions by performing retroviral rescue experiments. FO B cells from *Cd23*-Cre *Tcf3,4*$^{fl/fl}$ or *Aicda*$^{-/-}$ mice were infected with an empty retrovirus (MiCD2) expressing the human CD2 indicator protein or with retroviruses additionally expressing E2A (MiCD2-E2A), E2-2 (MiCD2-E2-2), or AID (MiCD2-AID). Flow cytometric analysis of the infected hCD2^{+} B cells at day 4 after LPS and IL-4 stimulation revealed that CSR to IgG1 and IgE was rescued by expression of E2A and E2-2 in DKO B cells, but not in *Aicda*$^{-/-}$ B cells, as expected (Fig. 6 C). Interestingly, AID expression restored CSR to IgG1 in activated DKO B cells, indicating that the loss of AID expression is the main reason for the absence of IgG1 CSR in these mutant B cells (Fig. 6 C). In contrast, AID expression could not rescue CSR to IgE in DKO cells (Fig. 6 C), as this switching process additionally depends on the E-protein–dependent expression of Iε GLTs (Fig. 5 E). Hence, these experiments further demonstrated that E2A and E2-2 control CSR by activating both *Aicda* expression and *Igh* germline transcription.

To investigate whether E-proteins are equally important for *Aicda* activation by different stimuli, we treated WT and DKO B cells for 3 d with different stimulation conditions before RT-qPCR analysis of *Aicda* mRNA. *Aicda* induction in response to anti-CD40, IL-4, and IL-5 or anti-CD40 and IL-4 stimulation required the presence of E2A and E2-2 (Fig. 6 D), consistent with the RNA-seq data of Fig. 6 A. Unexpectedly, *Aicda* expression was equally well induced in

Regulated E2A,E2-2 target genes were determined by overlapping E2A-bound genes (B, day 2) with E2A,E2-2-regulated genes (Fig. S1 F, day 3). The number and percentage of regulated E2A,E2-2 target genes are shown for the indicated fold gene expression differences between activated WT and DKO B cells. ND, not determined. (D) Functional classification and quantification (numbers) of the proteins encoded by the activated and repressed target genes identified in stimulated B cells. (E–H) Expression of activated E2A,E2-2 target genes coding for proteins involved in GC B cell formation (E), plasma cell differentiation (F), BCR signaling (G), and cell adhesion and migration (H). The expression of the indicated genes was determined by RNA-seq of ex vivo sorted WT GC B cells (orange) and bone marrow plasma cells (PC, black), as well as WT (gray) and DKO (green) FO B cells before (ex vivo) or after anti-CD40 and IL-4 stimulation for 1, 2, or 3 d. Gene expression was normalized as described in Fig. 1 A. All RNA-seq data are based on two experiments for each genotype and cell type, and the ChIP-seq data correspond to one experiment.

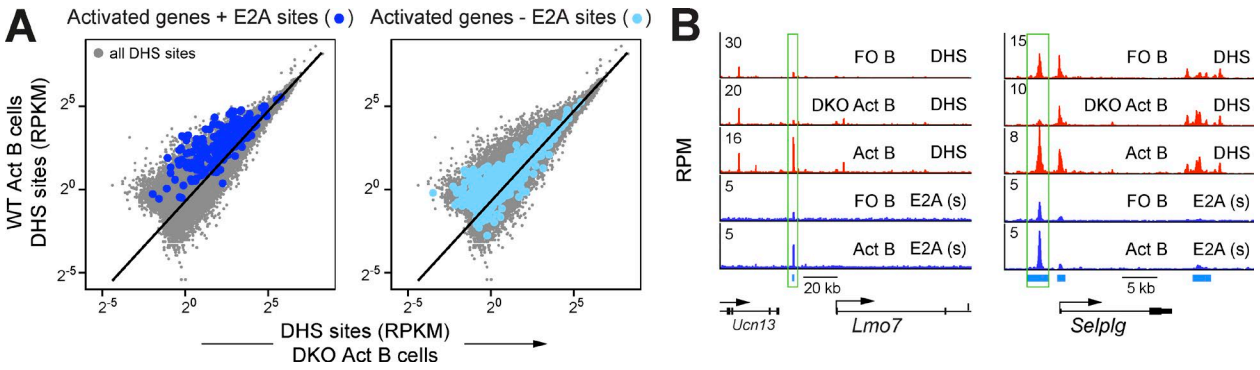

Figure 4. **E-protein–dependent formation and maintenance of DHS sites at activated target genes.** (A) DHS sites were mapped by ATAC-seq (Buenrostro et al., 2013) in WT and DKO B cells at day 2 of anti-CD40 and IL-4 stimulation, and the density of each DHS site was measured as RPKM value. A scatter plot of density differences between activated (Act) B cells of the WT and DKO genotypes is shown for all DHS sites (gray dots), DHS sites located at E2A peaks of activated genes (dark blue dots, left) and DHS sites lacking E2A binding at activated genes (light blue dots, right). The data are based on one ATAC-seq experiment for each cell type. (B) E2A-binding and DHS sites at the activated target genes *Lmo7* and *Selplg* in FO and activated B cells. E-protein–dependent DHS sites are boxed. The scales for visualizing DHS sites were adjusted to show equal densities of DHS sites at the ubiquitously expressed *Tbp* locus (Fig. S1 G).

DKO and WT B cells upon stimulation with anti-CD40 and IL-21 (Fig. 6 D). We next cultured DKO B cells on stromal 40LB cells (Nojima et al., 2011), expressing BAFF and the membrane-bound CD40 ligand, in the presence of IL-4 for 4 d, which failed to activate CSR to IgG1 (Fig. 6 E), consistent with the data of Fig. 5 B. In contrast, DKO B cells underwent efficient IgG1 CSR upon further stimulation with IL-21 (replacing IL-4) for another 4 d (Fig. 6 E). We conclude therefore that *Aicda* activation differs in the requirement for E2A and E2-2, depending on the stimulation conditions.

Loss of plasma cells in the absence of E2A and E2-2

Long-lived memory plasma cells ($CD138^+CD28^+B220^{int}Lin^-$; Delogu et al., 2006) were present at similar numbers in the bone marrow of nonimmunized *Cd23*-Cre *Tcf3*$^{fl/fl}$ (E2A KO), *Cd23*-Cre *Tcf3,4*$^{fl/fl}$ and control *Tcf3,4*$^{fl/fl}$ mice (Fig. 7 A). However, plasma cells were threefold reduced in the bone marrow of *Cd23*-Cre *Tcf4*$^{fl/fl}$ (E2-2 KO) mice (Fig. 7 A), indicating that E2-2 is the dominant E-protein consistent with its high expression in plasma cells (Fig. 1 A). Only half of all plasma cells in DKO mice expressed GFP (Fig. 7 A). Moreover, the second *Tcf3* allele was incompletely deleted and the intact floxed *Tcf4* alleles were retained in GFP^+ DKO plasma cells, as shown by PCR genotyping (Fig. 7 B). Hence, the strong counterselection against *Tcf3* and *Tcf4* deletion indicates an essential role for E2A and E2-2 in plasma cell development. Immunization with the T cell–independent antigen TNP-Ficoll resulted at day 14 in a significant reduction of plasma cells in the spleen of both E2A KO and E2-2 KO mice. Although the DKO plasma cells were present in higher numbers, they largely failed to express GFP, further indicating efficient counterselection against the combined loss of E2A and E2-2 in plasma cells (Fig. 7 C). A similar picture was observed at day 14 after immunization with the T cell-dependent antigen NP-KLH (Fig. 7 D), which also demonstrated incomplete *Tcf3* deletion and retention of the intact floxed *Tcf4* alleles in GFP^+ DKO plasma cells (Fig. 7 E). Hence, E2A and E2-2 are essential regulators of plasma cell development.

Loss of E2A and E2-2 arrests plasmablast differentiation at an activated B cell stage

We next investigated the role of E2A and E2-2 in an in vitro plasmablast differentiation system. For this, FO B cells from WT mice were stimulated with LPS for 4 d, which generated activated B cells ($CD22^+CD138^-$), preplasmablasts ($CD22^-CD138^-$), and plasmablasts ($CD22^-CD138^+$; Minnich et al., 2016; Fig. 8 A). In contrast, LPS-induced differentiation of DKO B cells resulted in a major $CD22^+CD138^-$ cell population with high GFP expression and in a small population (0.6%) of DKO plasmablasts, which was largely GFP^- and thus failed to delete *Tcf3* (Fig. 8 A). Notably, the DKO B cells exhibited only a minor decrease in proliferation (Fig. 8 B), but contained 10-fold less anti-IgM–secreting cells compared with WT cells (Fig. 8 C). Collectively, these results demonstrate that the loss of E2A and E2-2 stringently arrests plasmablast differentiation at a $CD22^+CD138^-$ cell stage.

We next performed RNA-seq with activated WT and DKO B cells at day 2 of LPS stimulation (Fig. S3 A), and with activated WT B cells, preplasmablasts, plasmablasts, and the arrested DKO cells at day 3 of LPS stimulation (Fig. S3 B). Principal component analysis of these RNA-seq data demonstrated that the DKO cells were most closely related to the activated WT B cells (Fig. 8 D). Moreover, the B cell–specific genes *Pax5*, *Spib*, *Bcl11a*, *Cd22*, and *Cd40*, which are normally repressed during plasmablast differentiation, were still highly expressed in the DKO cells (Fig. S4 A). Together, these findings indicate that the loss of E2A and E2-2 blocks LPS-induced differentiation at an activated B cells stage before the onset of plasmablast formation.

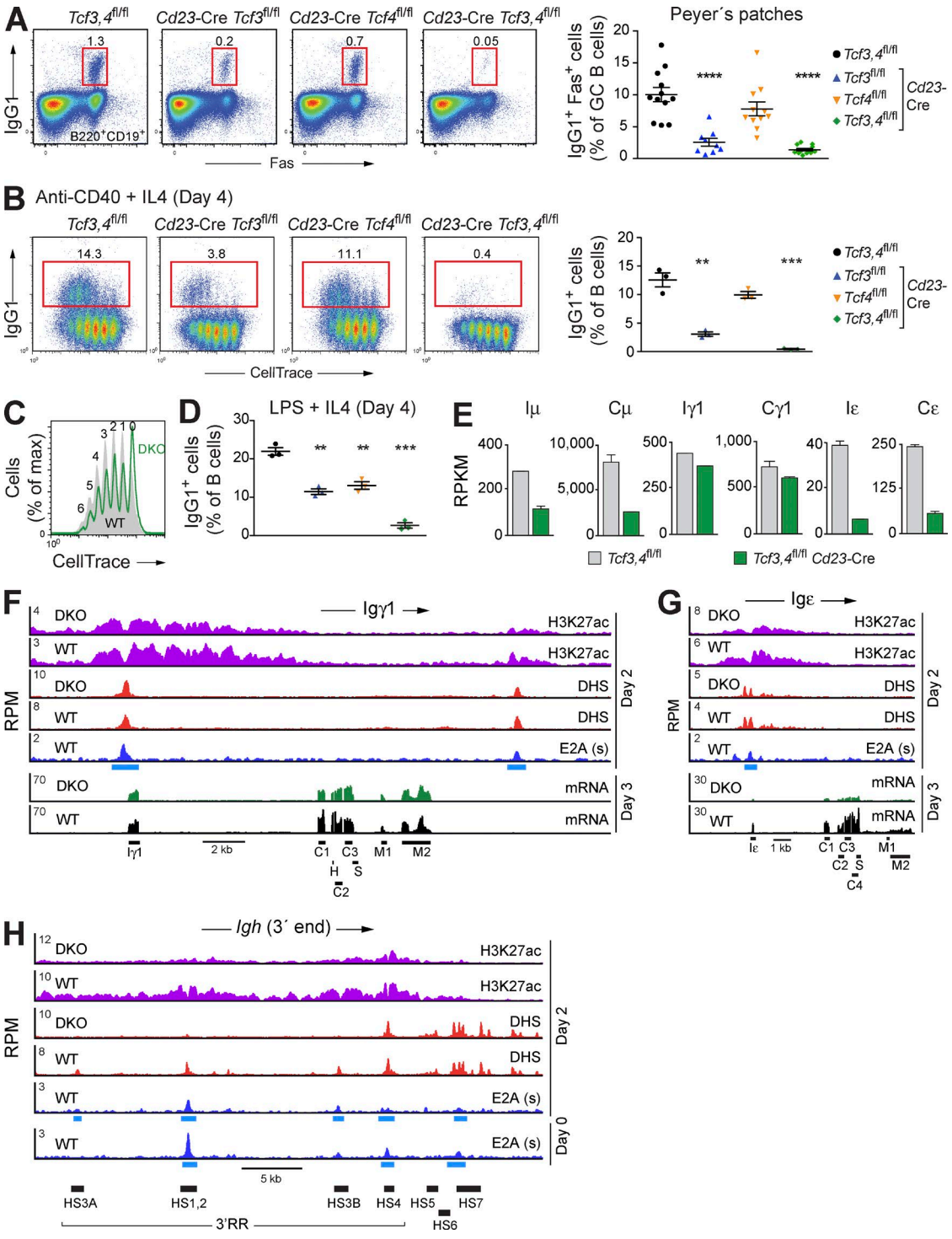

Figure 5. **E2A and E2-2 regulate CSR by controlling enhancers in the 3′RR of the *Igh* locus.** (A) Flow cytometric analysis of IgG1$^+$Fas$^+$ GC B cells in Peyer's patches of the indicated genotypes. To the right, the percentages of IgG1$^+$Fas$^+$ B cells relative to all Fas$^+$ GC B cells of individual mice are shown as statistical data with SEM. **, $P < 0.01$; ***, $P < 0.001$; ****, $P < 0.0001$, (Student's *t* test) calculated relative to the *Tcf3,4*$^{fl/fl}$ genotype (left). Each symbol represents one mouse, and the data are pooled from six experiments. (B and C) IgG1 CSR in response to anti-CD40 and IL-4 stimulation. CD43$^-$ FO B cells from lymph nodes of the indicated genotypes were stained with the CellTrace Violet reagent before stimulation with anti-CD40 and IL-4 for 4 d. The relative percentage of IgG1$^+$ B cells was analyzed (B, left) and quantified by statistical analysis (B, right) as described in A. Each symbol represents a stimulation experiment performed with B cells from one mouse (B). The data are shown for one of two experiments. CellTrace staining revealed the proliferation and divisions of WT (gray) and DKO (green) B cells (C). (D) IgG1 CSR of lymph node B cells stimulated with LPS and IL-4 for 4 d. Flow cytometric data were

Analysis of the RNA-seq data of activated WT and DKO cells resulted in 41 activated and 45 repressed genes in activated B cells at day 2, as well as in 127 activated and 106 repressed genes at day 3 of LPS stimulation (Fig. S3, C and D). ChIP-seq analysis further revealed 4,092 E2A-bound target genes in LPS-activated B cells at day 2, as well as 5,488 and 6,985 E2A target genes in LPS-differentiated preplasmablast and plasmablasts at day 4, respectively (Fig. S3, E–I). By determining the overlap between the E2A,E2-2-regulated genes (Fig. S3 D) and E2A-bound genes (Fig. S3 I), we identified 110 potentially directly activated and 42 potentially directly repressed E2A,E2-2 target genes in activated B cells at day 3 of LPS stimulation (Fig. 8 E and Table S2). Whereas both anti-CD40 plus IL-4 and LPS stimulation conditions defined a common set of 33 activated E2A,E2-2 target genes, only three repressed target genes were common to both treatments (Fig. 8 F). Moreover, 46% of all activated target genes code for 14 surface receptors, 17 signal transducers, 16 transcriptional regulators, and 4 proteins involved in ER function (Fig. 8 G). We further divided the activated target genes of these four classes according to their expression during plasmablast differentiation. Activated target genes, which were not at all or only weakly up-regulated during plasmablast differentiation, code for 12 cell surface receptors (Tbxa2r, Slamf7, Plxnd1, Il9r, Cd2, Sdc4, Il6ra, Crim1, Cxcr4, Sell [CD62L], Gpr183 [EBI2], and Cd9), 10 signal transducers (Sit1, Rap1gap2, Pik3r5, Sik1, Rasgrp2, Pim1, Ticam2, Spred2, Map3k8, and Ralgds), and 8 transcriptional regulators (Id3, Cbfa2t3, Trp73, Id2, Mef2b, Bhlhe41, Hivep3, and Sox4; Fig. S4, B–D). The second class of activated target genes was more than threefold up-regulated during plasmablast differentiation and codes for two cell surface receptors (Ccr9 and Itgb3), seven signal transducers (Gnaz, Irs2, Plcd3, Lax1, Dusp5, Dusp14, and Myzap), eight transcriptional regulators (Blimp1 [*Prdm1*], Xbp1, Eaf2, Bhlha15, Hes1, Cebpb, Creb3l2, and Cbx4), and four molecules involved in protein secretion and homeostatic control of the ER (Tram2, Edem3, Edem1, Wfs1; Fig. 8, H–K). It is important to note that the strong induction of these genes in activated B cells at day 3 of LPS stimulation cannot be explained by contaminating preplasmablasts, as nonregulated genes with high expression in preplasmablasts were similarly expressed in activated WT and DKO B cells (Fig. S4 E). Hence, the identified activated target genes likely contribute to the stringent arrest of plasmablast differentiation in the absence of E2A and E2-2.

E-protein–dependent control of 3′ enhancers at the *Igh* and *Igk* loci

We next studied the E-protein–dependent regulation of *Igh* and *Igk* gene expression in view of the fact that increased expression and secretion of immunoglobulins is a hallmark of plasma cells (Nutt et al., 2015). Whereas the expression of *Igh* and *Igk* transcripts was strongly increased during LPS-induced differentiation of activated B cells to plasmablasts, this increase was not observed in activated DKO cells (Fig. S5, A and B). Moreover, the mRNAs encoding the secreted $Ig\mu_s$, $Ig\gamma2b_s$, and $Ig\gamma3_s$ proteins were strongly increased in WT preplasmablasts and plasmablasts in contrast to activated DKO B cells, indicating that the posttranscriptional switch to the $Ig\mu_s$, $Ig\gamma2b_s$, and $Ig\gamma3_s$ transcripts did not take place in the absence of E2A and E2-2 (Fig. S5, B and C).

High expression of Ig heavy-chain proteins in plasma cells depends on the four enhancers (HS1/2, HS3A, HS3B, and HS4) in the 3′RR of the *Igh* locus (Vincent-Fabert et al., 2010). As shown by DHS site analysis, all four enhancers were already present in open chromatin in LPS-activated WT B cells (Fig. S5 D). In contrast, the accessibility at the HS3A, HS1,2, and HS3B enhancers was strongly reduced in activated DKO B cells (Fig. S5 D). Notably, E2A bound to all four enhancers in the 3′RR (Fig. S5 D). Hence, these data suggest that E2A and E2-2 are directly responsible for inducing open chromatin at the 3′RR in LPS-activated B cells, similar to the situation observed with anti-CD40 and IL-4–stimulated B cells (Fig. 5 H). Likewise, the loss of E2A and E2-2 in activated DKO B cells led to reduced chromatin accessibility at three E2A-bound enhancers (iE_κ, $3'E_\kappa$, and Ed) in the 3′ region of the *Igk* locus (Fig. S5 E). Hence, E-proteins regulate the activity of 3′ *Igh* and *Igk* enhancers in activated B cells.

Regulation of the *Prdm1* gene by a distant E-protein–dependent enhancer

Both LPS and anti-CD40 plus IL-4 stimulation identified *Xbp1* and *Prdm1* (Blimp1) as activated E2A,E2-2 target genes, which have important functions in plasma cells (Figs. 3 F and 8 I). The *Xbp1* locus, which codes for an essential regulator of immunoglobulin secretion (Reimold et al., 2001), was bound by E2A at several putative upstream enhancers, some of which lost their open chromatin in activated DKO cells (Fig. S5 F). As Blimp1 is an essential regulator of plasma cell development (Martins and Calame, 2008), we next investigated whether retroviral Blimp1 expression in DKO B cells

statistically analyzed as in A. Each symbol represents one mouse, and the data are shown for one of two experiments. (E) Expression of *Igh* transcripts in lymph node B cells stimulated with anti-CD40 and IL-4 for 3 d. The abundance of germline transcripts at the Iμ, Iγ1 and Iε exons and transcripts at the Cμ, Cγ1 and Cε exons is shown as average RPKM value of two RNA-seq experiments with SEM for each indicated genotype. (F-H) E-protein-dependent regulation of *Igh* constant gene segments and the 3′RR. DHS sites, active chromatin (H3K27ac), E2A binding and gene transcripts are shown for the Igγ1 (F) and Igε (G) gene regions and the 3′RR (H) in WT and DKO B cells at the indicated days of anti-CD40 and IL-4 stimulation. The intronic [I] promoters and the constant [C], hinge [H], secreted [S], and membrane [M] exons of the Igγ1 (F) and Igε (G) gene regions and the enhancers (HS3A, HS1,2, HS3B, and HS4) of the 3′ RR (H) are shown. The scales were adjusted to show equal H3K27ac or DHS site densities at the *Tbp* locus, respectively (Fig. S1 G).

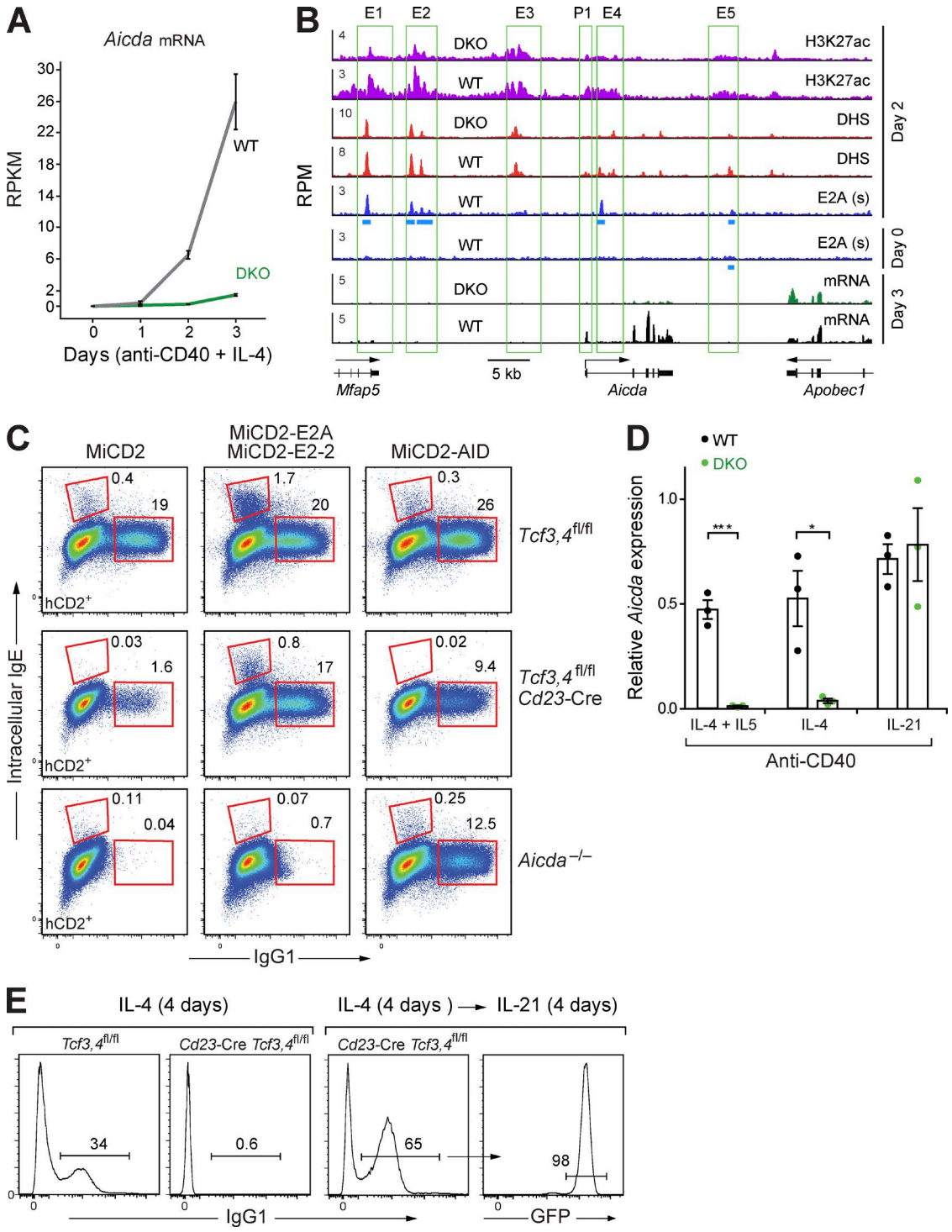

Figure 6. **Regulation of the *Aicda* gene by E2A and E2-2.** (A) *Aicda* expression at different days of anti-CD40 and IL-4 stimulation is shown as mean RPKM value with SEM for WT and DKO B cells, based on two RNA-seq experiments. (B) DHS sites, active chromatin (H3K27ac), E2A binding, and gene transcripts are shown for WT and DKO B cells at the indicated days of anti-CD40 and IL-4 stimulation. The *Aicda* gene is shown together with its promoter (P1) and five enhancer regions (E1–E5; Kieffer-Kwon et al., 2013). The scales were adjusted to show equal H3K27ac or DHS site densities at the *Tbp* locus, respectively (Fig. S1 G). (C) Lymph node FO B cells of the indicated genotypes were infected with the retrovirus MiCD2 or retroviruses expressing E2A (MiCD2-E2A), E2-2 (MiCD2-E2-2), or AID (MiCD2-AID) together with a human (h) CD2 indicator protein. The infected DKO B cells were cultured in the presence of LPS and IL-4 for 4 d before analysis of the cell surface IgG1 and hCD2 proteins combined with intracellular IgE staining. IgG1 and IgE expression is displayed for infected hCD2$^+$ B cells. One of three experiments is shown. (D) Lymph node FO B cells of the WT or DKO genotype were treated with the indicated stimuli for

could restore plasmablast formation. Lymph node B cells from *Tcf3,4*$^{fl/fl}$, *Cd23*-Cre *Tcf3,4*$^{fl/fl}$, and *Cd23*-Cre *Prdm1*$^{Gfp/fl}$ mice were infected with the control retrovirus MiCD2 or the retroviruses MiCD2-E2-2 or MiCD2-Blimp1, followed by flow cytometric analysis of the infected hCD2$^+$ B cells at day 4 after LPS stimulation (Fig. 9 A). As expected, E2-2 expression rescued the differentiation of DKO B cells to plasmablasts (Fig. 9 A), which efficiently secreted IgM antibodies (Fig. 9 B). Although retroviral Blimp1 expression could restore plasmablast differentiation of Blimp1 KO B cells, it was unable to restore the differentiation of E2A,E2-2–deficient DKO B cells to IgM-secreting plasmablasts (Fig. 9, A and B). Hence, Blimp1 expression is not sufficient to overcome the developmental arrest of activated DKO B cells.

Mapping of DHS sites in LPS-activated B cells and plasmablasts identified several potential enhancers in the upstream region of the *Prdm1* gene (Fig. 10 A). Whereas E2A bound weakly to some of these elements, the most prominent E2A-binding site was detected at a putative enhancer located 272-kb upstream of the *Prdm1* gene (Fig. 10 A). Importantly, the DHS site at this putative enhancer (referred to as site H) was lost in activated DKO B cells (Fig. 10 A). To determine a potential interaction between the *Prdm1* promoter and DHS site H, we analyzed the three-dimensional (3D) architecture of the *Prdm1* locus by performing chromosome conformation capture (3C) experiments with LPS-stimulated WT plasmablasts and in vitro–cultured control pro–B cells. The 3C-qPCR analysis was performed with primers located in the reference HindIII fragment at the *Prdm1* promoter and in HindIII fragments containing different upstream DHS sites (Fig. 10 B). Relative cross-linking frequencies that were high in plasmablasts and low in pro–B cells identified long-range interactions between the *Prdm1* promoter and the DHS sites B (−145 kb), C (−170 kb), D (−230 kb), F (−250 kb), and H (−272 kb) in plasmablasts (Fig. 10 B). To determine a possible role of the E2A-binding site at DHS site H in long-range looping, we generated a mouse carrying a 3-bp mutation (Mut) in the consensus E2A-binding sequence of DHS site H by CRI SPR/Cas9-mediated genome engineering (Fig. 10 C). E2A binding to the mutated DHS site H was reduced by sixfold but not abolished in *Prdm1*$^{Mut/Mut}$ plasmablasts (Fig. 10 D). Notably, the partial loss of E2A binding specifically reduced the long-range interaction of DHS site H with the *Prdm1* promoter in *Prdm1*$^{Mut/Mut}$ plasmablasts (Fig. 10 B) and resulted in a significant decrease of nascent *Prdm1* transcripts in *Prdm1*$^{Mut/Mut}$ preplasmablast and plasmablasts (Fig. 10 E). We therefore conclude that E-proteins contribute to the 3D architecture of the *Prdm1* locus and regulate *Prdm1* transcription by activating the distal enhancer H.

DISCUSSION

E2A is an essential regulator of early B cell development (Murre, 2005; Kwon et al., 2008). Here, we have demonstrated that E2A cooperates with E2-2 in regulating late B cell development and B cell immunity, as both transcription factors are strictly required for the development of GC B cells and plasma cells in response to immunization. E2A proved to be the dominant E-protein for GC B cell differentiation, and E2-2 was more important for plasma cell development, in agreement with their relative expression in the two cell types.

The main function of E2A and E2-2 in activated B cells appears to be transcriptional activation rather than repression, as indicated by the fact that E2A bound to most activated genes in contrast to only one third of the repressed genes. Moreover, few repressed target genes were highly regulated by the two E-proteins in contrast to a large proportion of the activated target genes. In support of transcriptional activation, E-proteins contain 3 activation domains (AD1, AD2, and AD3), which interact with the coactivators p300 and CBP (Bradney et al., 2003; Bayly et al., 2004) and the promoter recognition factor TFIID (Chen et al., 2013). At the chromatin level, we identified a novel role for E-proteins in shaping the enhancer landscape at its activated target genes, as E2A and E2-2 are responsible for the induction and maintenance of DHS sites containing E2A-binding sites. This novel function, which is best exemplified by the E-protein–dependent enhancers located at the *Aicda* locus and in the 3′ regions of the *Igh* and *Igk* loci, may be mediated by recruitment of the histone acetyltransferases p300 and CBP to E2A-binding sites at activated target genes.

Conditional E2A loss in mature B cells is known to impair the development of GC B cells (Kwon et al., 2008). Here, we demonstrate that the combined loss of E2A and E2-2 entirely prevents GC B cell development. The loss of GC B cells is likely explained by the reduced expression of the activated E2A,E2-2 target genes *Icosl*, *Pou2af1*, and *Mef2b*. GC formation strictly depends on the interplay between Tfh and B cells, which is mediated by interaction of the ICOS receptor on Tfh cells with the ICOS ligand (*Icosl*) on B cells (Nurieva et al., 2008). GC B cells also fail to develop in the absence of the transcriptional co-activator OBF-1/OCA-B (*Pou2af1*; Schubart et al., 1996; Qin et al., 1998). Finally, the transcription factor MEF2B (*Mef2b*) was shown to directly activate the *Bcl6* gene, which itself codes for an essential regulator of GC B cell development (Ying et al., 2013).

Retroviral overexpression of ID3 in activated B cells implicated E-proteins in the control of CSR (Quong et al., 1999) and AID expression (Sayegh et al., 2003). Here, we have significantly extended these findings by demonstrat-

3 d and sorted as large CD22$^+$CD138$^-$ cells before RT-qPCR analysis of *Aicda* mRNA. Symbols represent the analysis of three mice for each genotype in one experiment. Statistical data are shown with SEM. *, $P < 0.05$; ***, $P < 0.001$, Student's *t* test. (E) WT and DKO splenic B cells were co-cultured on stromal 40LB cells (Nojima et al., 2011) with IL-4 for 4 d, and the stimulated DKO B cells were subsequently cultured with IL-21 (instead of IL-4) for another 4 d before flow cytometric analysis. The data are shown for one of two experiments.

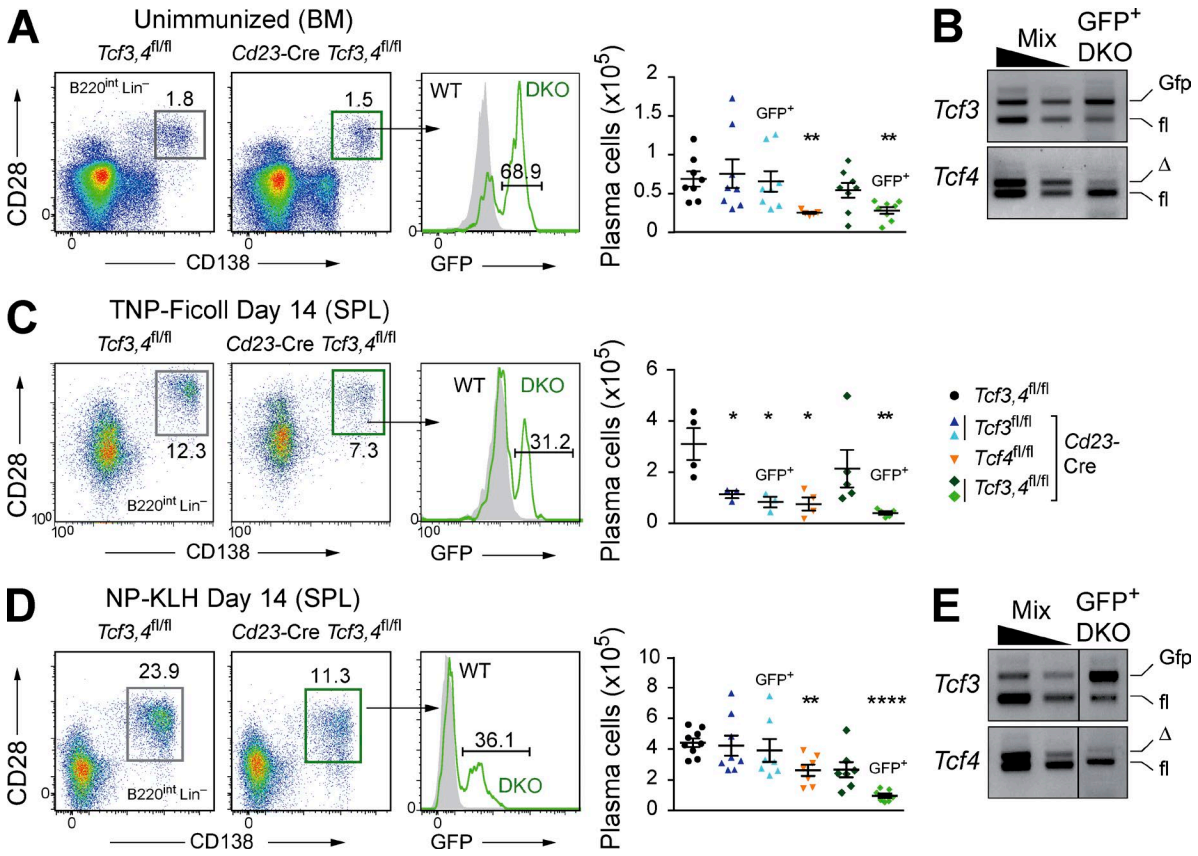

Figure 7. **Loss of plasma cells in the absence of E2A and E2-2.** (A and B) Plasma cells in nonimmunized mice. Plasma cells in the bone marrow (femur and tibia of the two hind legs) of the indicated genotypes were identified as Lin$^-$B220^{int}CD28$^+$CD138$^+$ cells (A, left), and their absolute cell numbers were determined (A, right). Statistical data are shown with SEM. *, $P < 0.05$; **, $P < 0.01$; ***, $P < 0.001$; ****, $P < 0.0001$ (Student's *t* test) calculated relative to the *Tcf3,4*$^{fl/fl}$ genotype (left). Each symbol represents one mouse, and the data are pooled from three experiments. (B) PCR detection of *Tcf3* and *Tcf4* deletion in sorted GFP$^+$ plasma cells from the bone marrow of a DKO mouse, as described in Fig. 1 C. (C–E) Plasma cells in mice immunized with the T cell–independent antigen TNP-Ficoll (C) or T cell–dependent NP-KLH (D and E). Splenic plasma cells were analyzed at day 14 after immunization and were statistically evaluated, as described in A. The data are from one experiment (C) or pooled from two experiments (D). (E) PCR analysis of *Tcf3* and *Tcf4* deletion in sorted GFP$^+$ plasma cells from a DKO spleen, as described in Fig. 1 C.

ing that E-proteins control CSR by regulating *Igh* germline transcription through the 3′RR domain and by controlling *Aicda* expression through multiple enhancers. E2A controls three of the four enhancers at the *Igh* 3′RR in activated B cells, as shown by the following evidence. First, E2A bound to all four enhancers. Second, the DHS sites were strongly reduced or lost at three enhancers (HS3A, HS1,2, and HS3B) in activated DKO B cells. Third, active chromatin (H3K27ac) was strongly decreased in the entire 3′RR domain, possibly as a result of inefficient recruitment of the histone acetyltransferases p300 and CBP in the absence of E2A and E2-2. The loss of 3′RR enhancer activity likely explains the strong decrease of Iε germline transcription in DKO B cells stimulated with anti-CD40 and IL-4. Surprisingly however, Iγ1 germline transcription was minimally influenced by the loss of both E-proteins, consistent with the observation that deletion of the entire 3′RR leads to a relatively small decrease of Iγ1 GLTs and a partial loss of IgG1 CSR (Vincent-Fabert et al., 2010; Saintamand et al., 2015). In agreement with this finding, retroviral restoration of AID expression in DKO B cells was sufficient to rescue CSR to IgG1, but not to IgE, demonstrating that IgE CSR requires the E-protein–dependent activation of both the 3′RR enhancers and *Aicda* gene.

The *Aicda* locus contains five distinct enhancer regions (E1-E5), which interact with each other and the *Aicda* promoter to form a local promoter-enhancer interactome that functions as one cooperative regulatory unit to induce *Aicda* expression (Kieffer-Kwon et al., 2013). In support of this idea, each enhancer is essential for efficient *Aicda* induction (Crouch et al., 2007; Huong et al., 2013; Kieffer-Kwon et al., 2013). Here we have demonstrated that E-proteins bind to four *Aicda* enhancers (E1, E2, E4, and E5) and contribute to *Aicda* regulation by establishing active chromatin and DHS sites at these enhancers.

The loss of plasma cells in *Cd23*-Cre *Tcf3,4*$^{fl/fl}$ mice identified a novel role for E-proteins in terminal B cell dif-

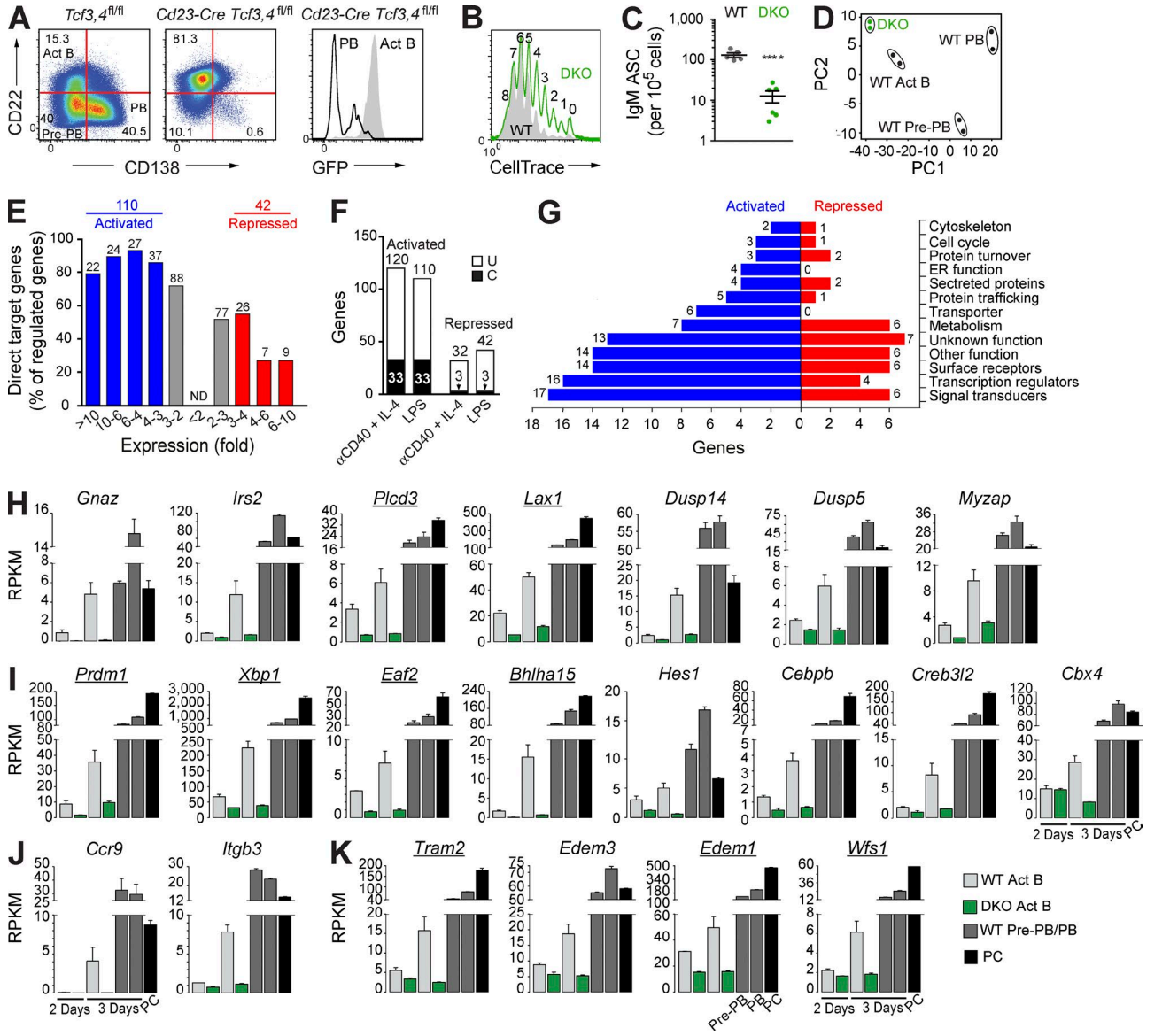

Figure 8. **Stringent block of plasmablast differentiation in the absence of E2A and E2-2.** (A) In vitro plasmablast differentiation. CD43⁻ FO B cells from lymph nodes of WT and DKO mice were stained with the CellTrace Violet reagent before LPS stimulation for 4 d. GFP expression is shown for activated B cells (Act B) and plasmablasts (PB) of the DKO genotype. Pre-PB, preplasmablasts. (B) The proliferation and divisions of WT (gray) and DKO (green) B cells, as revealed by CellTrace staining. (C) Reduced numbers of IgM ASCs without E2A and E2-2. CD43⁻ FO B cells of the WT or DKO genotype were stimulated with LPS for 4 d, followed by ELISPOT analysis of the entire cell population. Each dot represents the analysis of cells from one mouse. The data are pooled from two experiments. (D) Principal component analysis based on two RNA-seq experiments (day 3 of LPS stimulation) for each of the four cell types indicated. (E) Activated and repressed E2A,E2-2 target genes in activated B cells at day 3 of LPS stimulation. Regulated E2A,E2-2 target genes were determined by overlapping the E2A-bound genes (Fig. S3 I, day 2) with the E2A,E2-2-regulated genes (Fig. S3 D, day 3). The number and percentage of regulated E2A,E2-2 target genes are shown for the indicated fold gene expression differences between activated WT and DKO B cells. (F) Overlap of activated and repressed target genes at day 3 of LPS and anti-CD40 plus IL-4 stimulation. Common (C) and unique (U) genes are indicated. (G) Functional classification of proteins encoded by activated and repressed target genes. (H–K) Expression of activated E2A,E2-2 target genes that are up-regulated by greater than threefold in the transition from activated B cells to plasmablasts at day 3 of LPS stimulation. The expression of genes coding for cell surface receptor (J), signal transducers (H), transcriptional regulators (I), and proteins involved in ER function (K) is shown for activated WT (gray) and DKO (green) B cells, as well as for WT preplasmablasts (dark gray), plasmablasts (dark gray), and bone marrow plasma cells (PC, black). Gene expression is shown as mean RPKM value with SEM. Common target genes identified by anti-CD40 plus IL-4 and LPS stimulation are underlined. All RNA-seq data are based on two experiments for each genotype and cell type.

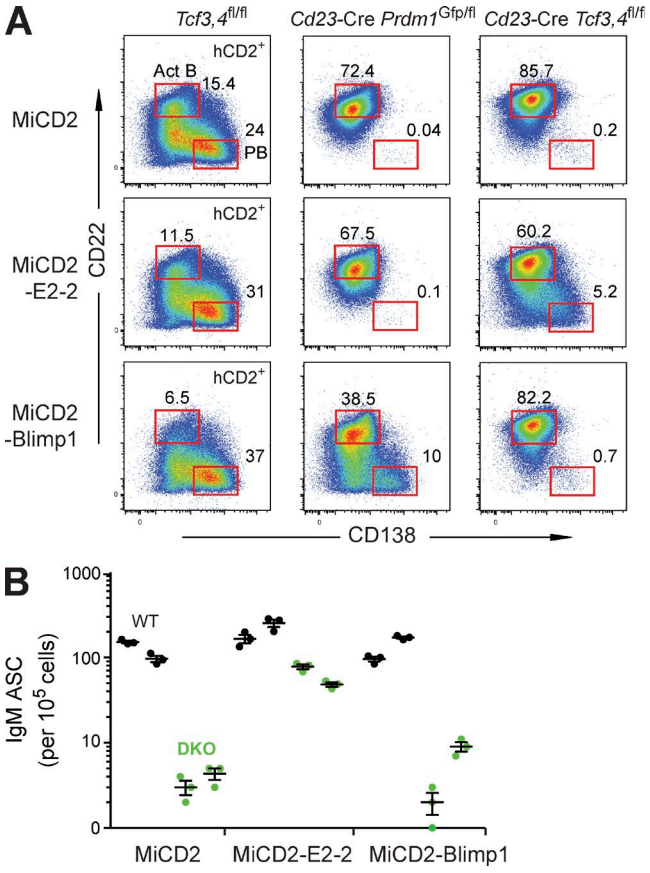

Figure 9. **Blimp1 expression does not recue plasmablast differentiation of E2A, E2-2–deficient B cells.** (A) Retroviral infection experiments. Lymph node FO B cells of the indicated genotypes were infected with the retrovirus MiCD2, MiCD2-E2-2, or MiCD2-Blimp1 and stimulated with LPS for 4 d before flow cytometric analysis. Only infected hCD2$^+$ B cells are shown. One of five experiments is shown. (B) ELISPOT analysis. Retrovirally infected FO B cells of two WT and two DKO mice were cultured with LPS for 4 d, followed by ELISPOT analysis of the unfractionated cell population. Each symbol corresponds to one well (containing 10^5 cells) of the ELISPOT analysis. Data are shown for one of two experiments.

ferentiation. The strict dependency of plasma cell development on E2A and E2-2 is best documented by the strong counterselection against *Tcf3* and *Tcf4* deletion in the residual plasma cells of *Cd23*-Cre *Tcf3,4*$^{fl/fl}$ mice. Moreover, the loss of E2A and E2-2 stringently arrests LPS-induced plasmablast differentiation at an activated B cell stage. Whereas plasmablasts and plasma cells are characterized by a high rate of immunoglobulin secretion (Nutt et al., 2015), the arrested DKO B cells fail to up-regulate *Igh* and *Igk* transcription and to undergo the posttranscriptional expression switch from the membrane-bound to secreted immunoglobulin heavy-chain. The inability to further activate *Igh* gene transcription is likely caused by the observed loss of open chromatin at the three *Igh* 3′ enhancers HS3A, HS1,2, and HS3B in activated DKO B cells. E2A was originally discovered as a DNA-binding protein interacting with the iE$_\kappa$ enhancer (Murre et al., 1989). Later, E2A was shown to regulate V$_\kappa$-J$_\kappa$ rearrangement in pre–B cells (Inlay et al., 2004). Here, we have demonstrated an important role for E2A and E2-2 in the control of *Igk* gene transcription by inducing DHS sites at the iE$_\kappa$, 3′E$_\kappa$, and Ed enhancers in LPS-activated B cells. This evidence strongly suggests that E-proteins contribute to the strong up-regulation of immunoglobulin expression in plasmablasts and plasma cells by establishing functional enhancers at the 3′ end of the *Igh* and *Igk* loci in activated B cells, consistent with the requirement of an intact 3′RR for promoting high secretion of Ig heavy-chain proteins in plasma cells (Vincent-Fabert et al., 2010).

Five transcription factors, IRF4, Aiolos, Ikaros, Blimp1, and XBP1, are currently known to play essential roles in plasma cell development, in addition to the E-proteins described here (Nutt et al., 2015). Of these transcription factor genes, only *Xbp1* and *Prdm1* (Blimp1) are directly activated by E2A and E2-2. As XBP1 is required for antibody secretion, but not for plasmablast differentiation (Taubenheim et al., 2012), its loss cannot account for the E-protein–dependent block of plasma cell development. In contrast, loss of Blimp1 stringently arrests plasmablast differentiation at an early stage (Shapiro-Shelef et al., 2003; Kallies et al., 2007). Although we identified E2A binding at multiple DHS sites in the 5′ region of the *Prdm1* locus, the most prominent E2A-binding region was detected at DHS site H, located 272-kb upstream of the *Prdm1* promoter. This distal DHS site is not only lost in activated DKO B cells, but also interacts with the *Prdm1* promoter. Importantly, mutation of a consensus E2A-binding sequence in DHS site H reduced not only the long-range interaction with the promoter, but also decreased *Prdm1* transcription, indicating that DHS site H functions as a distal enhancer to activate the *Prdm1* gene in plasmablasts. Retroviral restoration of Blimp1 expression in DKO B cells was, however, not sufficient to rescue plasmablast differentiation in the absence of E2A and E2-2, indicating that the reduced expression of some of the other 109 activated E2A,E2-2 target genes in DKO B cells also contributes to the differentiation block. Hence, E-proteins regulate plasma cell development in a pleiotropic manner, possibly as a result of their important function in shaping the enhancer landscape at their target genes during terminal B cell differentiation.

MATERIALS AND METHODS

Mice. The *Tcf3*$^{fl/fl}$ mice (Kwon et al., 2008), *Tcf4*$^{fl/fl}$ mice (Bergqvist et al., 2000), *Prdm1*$^{fl/fl}$ mice (Ohinata et al., 2005), *Prdm1*$^{Gfp/+}$ mice (Kallies et al., 2004), *Aicda*$^{-/-}$ mice (Muramatsu et al., 2000), and transgenic *Cd23*-Cre mice (Kwon et al., 2008) were maintained on the C57BL/6 genetic background. All animal experiments were performed according to valid project licenses, which were approved and regularly controlled by the Austrian Veterinary Authorities.

Generation of *Prdm1*$^{Mut/Mut}$ mouse. The E2A-binding site in DHS site H was mutated in the endogenous *Prdm1* locus by

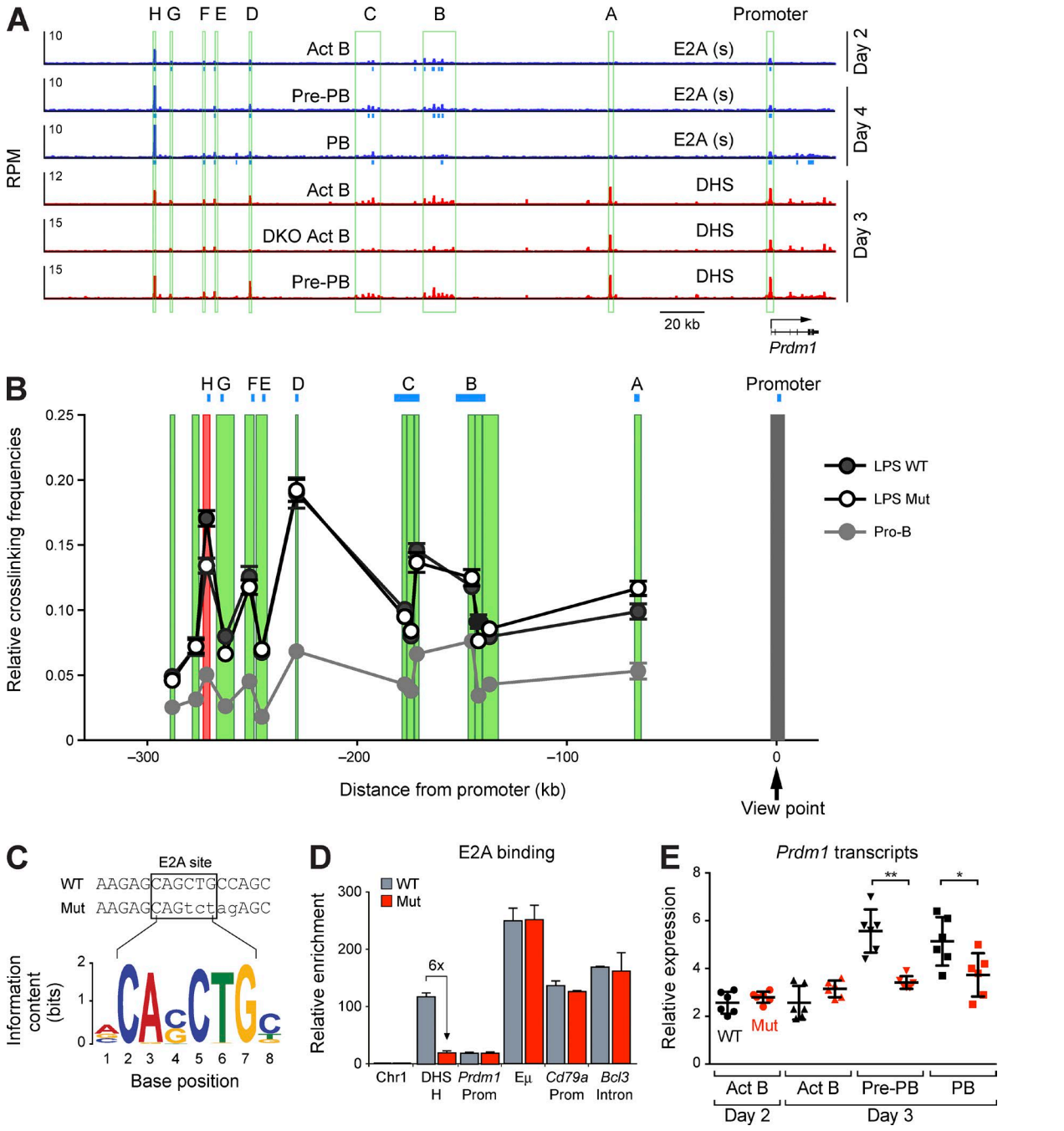

Figure 10. **Regulation of the *Prdm1* gene by E2A and E2-2.** (A) Mapping of E2A binding and DHS sites (labeled A to H) at the *Prdm1* locus in WT activated B cells (Act B), preplasmablasts (Pre-PB), and plasmablasts (PB), as well as activated DKO B cells at the indicated days of LPS stimulation. The scales of the DHS sites were adjusted to reveal equal densities at the *Tbp* locus (Fig. S1 G). (B) 3C-qPCR analysis of long-range interactions between the *Prdm1* promoter and upstream DHS sites. The relative cross-linking frequencies between the reference HindIII fragment at the *Prdm1* promoter and HindIII fragments containing the indicated DHS regions were determined with independently prepared 3C-templates. The mean cross-linking frequency with SEM is shown for each pair of HindIII fragments. WT and $Prdm1^{Mut/Mut}$ (Mut) FO B cells were differentiated for 4 d with LPS, and $Rag2^{-/-}$ pro-B cells were cultured for 4 d with IL-7 on OP9 cells before 3C-template preparation. The following independent 3C-templates were prepared; pro-B cells, 14 (from three mice); LPS-stimulated WT B cells, 21 (from four mice); LPS-stimulated Mut B cells, 19 (from three mice). The data are pooled from three 3C experiments. (C) Mutation of the E2A-binding site (position 44,454,501-6 on mouse Chr10, mm9) in DHS site H. The mutated nucleotides are shown in lowercase letters together with the consensus E2A-binding motif (E-value of 1.2×10^{-256}) identified at E2A peaks in plasmablasts. (D) Reduced E2A binding at the mutant DHS site H. WT and $Prdm1^{Mut/Mut}$ FO B cells were stimulated for 4 d with LPS before ChIP analysis with an E2A antibody. Input and precipitated DNA were quantified by real-time PCR with primers amplifying the E2A-binding regions of the indicated genes, and the amount of precipitated DNA was determined

CRISPR-Cas9–mediated genome editing (Yang et al., 2013). For this, Cas9 mRNA was co-injected with a specific sgRNA (linked to the scaffold tracrRNA) and a single-stranded repair oligonucleotide (171 nucleotides) into mouse zygotes (C57BL/6 x CBA), as previously described (Yang et al., 2013). The sgRNA, repair oligonucleotide, and PCR genotyping primers are shown in Table S3. The 1,056-bp PCR product amplified from the *Prdm1*^{Mut} allele was cleaved with XbaI, yielding 586-bp and 470-bp fragments, in contrast to the PCR fragment of the WT allele.

Antibodies. The following monoclonal antibodies were used for flow cytometric analysis of mouse spleen, lymph node, and bone marrow: B220/CD45R (RA3-6B2), CD4 (GK1.5), CD8a (53–6.7), CD11b/Mac1 (M1/70), CD19 (1D3), CD21/CD35 (7G6), CD22 (Cy34.1), CD23 (B3B4), CD28 (37.51), CD38 (90), CD49b (DX5), CD95/Fas (Jo2), CD138 (281–2), F4/80 (CI:A3-1), GL7 (GL-7), IgD (11.26c), IgE (R35-72), IgG1 (A85-1), IgG2b (R12-3), IgG3 (R40-82), IgM (II/41), and human CD2 (RPA-2.10) antibodies.

The rabbit polyconal anti-H3K27ac antibody (ab4729; Abcam) was used for ChIP experiments, and a rabbit polyconal anti-E2A antibody (Kwon et al., 2008) was used for ChIP and immunoblot analysis. The anti-E2A antibody (produced in-house) was directed against the N-terminal peptide DRP SSGSWGSSDQNSSSFDP of the mouse E2A protein, which is absent in the HEB and E2-2 proteins.

Definition and flow cytometric sorting of B cells, plasmablasts, and plasma cells. Mature B cells from lymph nodes, long-lived plasma cells from the bone marrow and in vitro–differentiated activated B cells and plasmablasts were sorted with a FACSAria machine (BD) as follows: immature B ($B220^+CD19^+IgM^{hi}IgD^{lo}CD21^-$), mature B ($B220^+CD19^+IgM^{lo}IgD^{hi}$), FO B ($B220^+CD19^+CD21^{int}CD23^{hi}$), MZ B ($B220^+CD19^+CD21^{hi}CD23^{lo/-}$), B-1 ($B220^{lo}CD19^+$), GC B ($B220^+CD19^+GL7^+Fas^+$), plasma cells ($Lin^-B220^{int}CD138^{hi}CD28^+$), in vitro–activated B cells ($CD22^+CD138^-$), preplasmablasts ($CD22^-CD138^-$), and plasmablasts ($CD22^-CD138^+$). The Lin marker antibodies contained anti-CD4, anti-CD8a, anti-CD11b, anti-CD21, and anti-DX5 antibodies for the analysis of plasma cells.

In vitro B cell stimulation experiments. FO B cells from the lymph nodes (RNA- and ATAC-seq) or spleen and lymph nodes (E2A-ChIP and 3C analyses) were isolated as $CD43^-$ B cells by immunomagnetic sorting. For LPS stimulation, FO B cells were seeded at a density of 5–50 × 10^4 cells/ml in IMDM medium containing 10% fetal calf serum (A15-101; GE Healthcare), 1 mM glutamine, 50 µM β-mercaptoethanol, and 25 µg/ml LPS (L4130; Sigma-Aldrich). For anti-CD40 plus IL-4 stimulation experiments, FO B cells were plated at 5 × 10^5 cells/ml in IMDM medium supplemented with 10% fetal calf serum, 1 mM glutamine, and 50 µM β-mercaptoethanol containing anti-CD40 antibody (2 µg/ml; HM40-3; eBioscience) and IL-4 (20 ng/ml) for up to 3 d. For cell proliferation analysis, the purified B cells were first stained with the CellTrace Violet reagent (5 µM; Invitrogen) before stimulation as described above. For LPS plus IL-4 stimulation, lymph node B cells were treated with LPS (25 µg/ml) and IL-4 (20 ng/ml) for 4 d. For the stimulation experiments shown in Fig. 6 D, the reagents were used at the following concentrations: anti-CD40 antibody (2 µg/ml), IL-4 (20 ng/ml), IL-5 (10 ng/ml), and IL-21 (10 ng/ml).

For experiments using the iGB system (Nojima et al., 2011), 40LB cells were cultured in DMEM medium supplemented with 10% fetal calf serum. Splenic B cells (10^5) were plated on irradiated 40LB feeder cells in one well of a 6-well plate in RPMI medium supplemented with 10% fetal calf serum, 1 mM glutamine, 50 µM β-mercaptoethanol, 10 mM Hepes, and 1 mM sodium pyruvate, followed by stimulation with IL-4 (20 ng/ml) for 4 d. At day 4, activated B cells (8 × 10^4) were transferred to fresh 40LB cells in one well of a 6-well plate and stimulated for another 4 d with IL-21 (10 ng/ml).

Immunization. Sheep RBCs (SRBCs) were washed in PBS and resuspended at 10^9 cells/ml, followed by intraperitoneal injection of 100 µl into an adult mouse. To study the immune responses to a T cell–independent antigen, mice were intraperitoneally injected with 10 µg of TNP (2,4,6-trinitrophenyl)-Ficoll (Biosearch Technology) in PBS. The immune response to a T cell–dependent antigen was investigated by intraperitoneal injection of 100 µg NP-KLH in alum.

ELISPOT analysis. The frequencies of IgM antibody-secreting cells (ASCs) were determined by enzyme-linked immunospot (ELISPOT) assay as described (Smith et al., 1997). Goat anti-mouse IgM antibody-coated plates were used for capturing IgM antibodies secreted by individual cells, respectively. Spots were visualized with goat anti-mouse IgM antibodies conjugated to alkaline phosphatase (Southern Biotech), and color was developed by the addition of BCIP/NBT Plus solution (Southern Biotech). After extensive washing, the spots were counted with an AID ELIspot reader system (Autoimmun Diagnostika).

as percentage relative to input DNA for each region. The enrichment relative to the negative control (Chr1) is shown as mean value with SEM based on two independent experiments. The data are pooled from two experiments. (E) RT-qPCR analysis of nascent *Prdm1* transcripts. LPS-stimulated WT and *Prdm1*$^{Mut/Mut}$ (Mut) cells were analyzed as unfractionated activated B cells (Act B) at day 2 or as sorted activated B cells, preplasmablasts, and plasmablasts at day 3. The amount of nascent *Prdm1* transcripts (intron 2) was normalized to the amount of nascent *Tbp* transcripts (intron 1). The mean value of six independent cell preparations (based on three mice per genotype) are shown with SEM. *, $P < 0.05$; **, $P < 0.01$, Student's *t* test. The data of one experiment are shown.

Histological analysis. Cryosections of the spleen from immunized mice were stained with a biotinylated anti-IgD antibody (1.19; produced in-house) and eFluor660-labeled GL7 antibody (GL-7; eBioscience). The biotinylated anti-IgD antibody was visualized by incubation with Cy3-streptavidin (Jackson ImmunoResearch Laboratories).

Cloning of retroviral expression constructs. For retroviral infection experiments, we cloned full-length mouse cDNA into the retroviral vector MiCD2 (Heavey et al., 2003) upstream of the IRES-hCD2 indicator gene to generate MiCD2-Blimp1, MiCD2-AID, MiCD2-V5-E2-2, and MiCD2-V5-E2A (containing full-length E47 cDNA). V5 refers to an N-terminal insertion of the V5 epitope tag.

Retroviral infection. Retroviruses were produced by transfecting 20 μg of the retroviral expression vector together with 10 μg of the retroviral helper vector pCMV-Gag-Pol into Plat-E packaging cells using standard calcium phosphate transfection in the presence of 25 μM chloroquine. 24 h after transfection, the high-titer viral supernatant was collected in B cell medium (IMDM supplemented with 10% fetal calf serum, 1 mM glutamine, and 50 μM β-mercaptoethanol). The infection was performed in a 6-well plate by spinning for 45 min at 2,400 rpm. Each well contained 10^6 lymph node B cells in 1 ml of freshly collected viral supernatant in B cell medium supplemented with LPS (25 μg/ml) or LPS (25 μg/ml) and IL-4 (20 ng/ml). The infection was repeated four times at intervals of 3–4 h in the presence of 4 μg/ml of polybrene except for the last infection. 4–12 h after the last infection, 5 ml of B cell medium containing LPS (25 μg/ml) and IL-4 (20 ng/ml) was added. The infected cells were analyzed 4 d after the start of culture.

RT-qPCR analysis of mRNA and nascent transcripts. Total RNA was prepared from sorted activated B cells, preplasmablasts, and plasmablasts by using the RNeasy Mini kit (QIA GEN). Genomic DNA was eliminated by using a gDNA eliminator spin column (QIAGEN). The cDNA was synthesized using the Random Primer Mix (New England Biolabs) and SuperScript III Reverse transcription (Life Technologies). *Aicda* transcripts were measured by qPCR using primers shown in Table S3, and were normalized against the *Tbp* transcripts. Nascent *Prdm1* transcripts were measured by qPCR using primers that are located in intron 2 (Table S3), and were normalized against nascent *Tbp* transcripts (intron 1).

3C-qPCR analysis. The 3C templates of activated B cells and plasmablasts or pro–B cells were prepared by using HindIII as the restriction enzyme as previously described (Medvedovic et al., 2013). DNA (200–400 ng) of individual 3C templates was subjected to quantitative TaqMan PCR analysis (qPCR; Hagège et al., 2007). The SensiFAST Probe No-ROX kit (Bioline Reagents Ltd.) was used for qPCR amplification, which was performed with the Bio-Rad CFX Connect Real-Time PCR Detection System using region-specific primers and a corresponding LNA Double-Dye probes with FAM and BHQ1 at the 5′ and 3′ ends, respectively (Table S3). As internal control for the quality of the 3C template, the ubiquitously expressed *Ercc3* (XPB) locus was analyzed by qPCR (Splinter et al., 2006). The cross-linking frequencies at the *Prdm1* and control *Ercc3* loci were calculated by using HindIII-digested and randomly ligated BAC DNA of these loci as a standard for PCR amplification. The relative cross-linking frequency was determined as the ratio of the cross-linking frequency at the *Prdm1* locus relative to the cross-linking frequency at the *Ercc3* gene.

Mapping of open chromatin regions. Open chromatin regions (referred to as DHS sites) were mapped in FO B cells, activated B cells and preplasmablasts by the ATAC-seq method as described (Buenrostro et al., 2013) with the following modification. The nuclei were prepared by incubating cells with nuclear preparation buffer (0.30 M sucrose, 10 mM Tris pH 7.5, 60 mM KCl, 15 mM NaCl, 5 mM $MgCl_2$, 0.1 mM EGTA, 0.1% NP-40, 0.15 mM spermine, 0.5 mM spermidine, and 2 mM 6AA) before the Tn5 treatment (4 μl of Nextera Tn5 transposase per 20,000 cells).

ChIP-seq analysis of histone modifications. For ChIP-seq analysis, activated B cells after 2 d of anti-CD40 plus IL-4 stimulation were used for ChIP with an anti-H3K27ac antibody (see Antibodies), as previously described (Schebesta et al., 2007). The ChIP-precipitated DNA (5 ng) was used for library preparation.

ChIP-seq analysis of E2A binding. In vitro–stimulated cells were subjected to cross-linking at room temperature either for 10 min with 1% formaldehyde (single cross-linking) or for 45 min with 2 mM disuccinimidyl glutarate (Sigma-Aldrich), followed by 10 min with 1% formaldehyde (double cross-linking). The chromatin was prepared as previously described (Kohwi-Shigematsu et al., 2012) with the following minor modifications. In brief, the nuclei were prepared from fixed cells before lysis with the 4% SDS solution. The lysed nuclei were subjected to 8M-urea gradient centrifugation (Kohwi-Shigematsu et al., 2012). The pelleted genomic DNA, cross-linked with proteins, were sheared with a Bioruptor sonicator (Diagenode) followed by immunoprecipitation using the anti-E2A antibody described in Antibodies. The ChIP-precipitated DNA (1–2 ng) was used for library preparation.

cDNA preparation for RNA sequencing. cDNA was prepared from RNA of in vitro–differentiated and ex vivo–sorted cells as previously described (Minnich et al., 2016).

Library preparation and Illumina deep sequencing. Approximately 1–5 ng of cDNA or ChIP-precipitated DNA were used as starting material for the generation of sequencing libraries

as described (Minnich et al., 2016). Table S4 provides detailed information about all sequencing experiments of this study.

Sequence alignment. Sequence reads that passed the Illumina quality filtering were considered for alignment. For ChIP-seq, the reads were aligned to the mouse genome assembly version of July 2007 (NCBI37/mm9), using the Bowtie program version 12.5. For alignment of ATAC-seq reads, the Bowtie version 2.1.0 was used with the additional parameter −sensitive −X 5000. For RNA-seq, the reads corresponding to mouse ribosomal RNAs (NCBI GenBank and RefSeq accession nos. BK000964.1 and NR_046144.1, respectively) were removed. The remaining reads were cut down to a read length of 44-nt and aligned to the mouse transcriptome (genome assembly version of July 2007 NCBI37/mm9) using TopHat version 1.4.1 (Trapnell et al., 2009).

Database of RefSeq-annotated genes. Peak-to-gene assignment and calculation of RNA expression values were all based on the RefSeq database, which was downloaded from UCSC on January 10th, 2014. The annotation of immunoglobulin and T cell receptor genes were incorporated from Ensembl release 67 (Cunningham et al., 2015). Genes with overlapping exons were flagged and double entries (i.e., exactly the same gene at two different genomic locations) were renamed. Identical genes with more than one assigned gene symbol were flagged. Genes with several transcripts were merged to consensus genes consisting of a union of all underlying exons using the fuge software, which resulted in 25,726 gene models.

Peak calling of E2A ChIP-seq data and target gene assignment. E2A peaks were determined in the following manner. First, peaks were called in the double-cross-linked E2A ChIP-seq sample with a p-value of $<10^{-10}$ and in the corresponding single-cross-linked E2A ChIP-seq sample with a p-value of $<10^{-5}$ by using the MACS program version 1.3.6.1 (Zhang et al., 2008) with default parameters, a genome size of 2,654,911,517 bp (mm9), and a mature B cell input sample (14,951). Second, the overlap of the called double- and single-cross-linked peaks was determined with the Multovl program (Aszódi, 2012) by using a minimal overlap length of one and allowing for all possible overlaps, with the results being parsed and converted to tables with custom-made bash, perl, and R scripts. The E2A peaks identified by this overlap analysis were then assigned to target genes as described (Revilla-i-Domingo et al., 2012). For comparisons of E2A ChIP-seq data between different cell types, we down-sampled the reads of all ChIP-seq experiments to the ChIP-seq experiment with the lowest number of aligned reads before peak calling.

Analysis of ATAC-seq data. The ATAC-seq data were analyzed as follows. The DHS sites (open chromatin) were identified by peak calling using the MACS 2.0.10 program. The peaks from WT and DKO cells were compiled. The peak regions were defined as peak summit ± 500 bp. Peaks were assigned to genes as described for the ChIP-seq analysis. The read density was calculated as RPKM value for each peak.

Read density heat maps. Read densities were calculated as previously described (Minnich et al., 2016).

Motif discovery. For motif discovery, we used the MEME-ChIP suite (version 4.9.1; Machanick and Bailey, 2011) to predict the most significant motifs present in the 300 bp centered at the peak summit of the top 300 sequences, as sorted by the fold enrichment score of the MACS program.

Analysis of RNA-seq data. For analysis of differential gene expression, the number of reads per gene was counted using HTseq version 0.5.3 (Anders et al., 2015) with the overlap resolution mode set to union. The datasets were grouped according to the performed stimulation experiments and analyzed using the R package DESeq2 version 1.4.1 (Love et al., 2014). Sample normalizations and dispersion estimations were conducted using the default DESeq2 settings. In detail, the following DESeq2 analyses were performed: FO B cell and all anti-CD40 and IL-4 stimulation samples were analyzed together considering the genotype, time and genotype over time effects (model design formula: "~genotype + time + genotype:time"). The genotype over time effect for each day was then tested based on log ratio tests (with a reduced formula of "~genotype + time"). FO B cell and 2-d LPS stimulation data were also grouped and analyzed in the same manner. 3-d LPS-stimulated activated B cell (WT and DKO), preplasmablast (WT), and plasmablast (WT) samples were considered for sample normalization, dispersion estimation, rlog normalization of the gene counts, and the comparison of 3-d LPS-stimulated DKO versus 3-d LPS-stimulated WT activated B cells (Wald test). The 500 most varying rlog normalized counts (option blind) of the 3-d LPS stimulation dataset were used for PCA in Fig. 8 D. In general, genes with an adjusted p-value <0.05 and a fold change >3, as well as a mean RPKM (averaged within conditions) >3 were considered to be significantly expressed. Immunoglobulin and T cell receptor genes were filtered from the list of significantly expressed genes and were also disregarded in the RPKM calculations.

For detailed expression analysis of the *Igh* and *Igk* loci (Figs. 5 E and S5, A and C), IghM, IghD, IghG, IghE, and IghA were manually curated to provide detailed exon annotations and were split into constant, membrane, secreted, hinge, and I exon regions. Ratios between secreted and membrane *Igh* transcripts were estimated by using the RPKM values of the secreted and membrane regions.

Accession nos. The RNA-seq, ChIP-seq, and ATAC-seq data (Table S4) are available at the Gene Expression Omnibus (GEO) repository under the accession no. GSE77744.

Online supplemental material. Figs. S1 and S3 describe the E2A-binding analysis of B cells stimulated with anti-CD40 plus IL-4 or LPS, respectively. Figs. S2 and S4 show the expression patterns of interesting E2A,E2-2 target genes identified in B cells stimulated with anti-CD40 plus IL-4 or LPS, respectively. Fig. S5 deals with the E-protein–dependent regulation of *Igh* and *Igk* during LPS-induced plasmablast differentiation. Tables S1 and S2 contain the RNA-seq data of all regulated E2A,E2-2 target genes identified in B cells stimulated with anti-CD40 plus IL-4 or LPS, respectively. Table S3 provides the oligonucleotide primer information. Table S4 describes all Illumina sequencing experiments generated for this study. Online supplemental material is available at http://www.jem.org/cgi/content/full/jem.20152002/DC1.

ACKNOWLEDGMENTS

We thank D. Holmberg (Umeå University) for providing *Tcf3*$^{fl/fl}$ mice, S.L. Nutt (WEHI Melbourne) for *Prdm1*$^{Gfp/+}$ mice, A. Tarakhovsky (Rockefeller University) for *Prdm1*$^{fl/fl}$ mice, D. Kitamura (Tokyo University) for 40LB cells, C. Theussl for blastocyst injection, K. Aumayr and her team for flow cytometric sorting and A. Sommer and his team (Vienna Biocenter Core Facility) for Illumina sequencing.

This research was supported by Boehringer Ingelheim, a European Research Council Advanced grant (291740-LymphoControl) from the European Union Seventh Framework Program, the Austrian Industrial Research Promotion Agency, and a German Research Foundation fellowship (WO 1972/1-1; M. Wöhner).

The authors declare no competing financial interests.

Author contributions: M. Wöhner did most experiments; H. Tagoh performed all E2A ChIP-seq, ATAC-seq, 3C-qPCR, and nascent transcript analyses; I. Bilic performed the initial phenotypic analyses; D. Kostanova Poliakova generated retroviral constructs and the *Prdm1*$^{Mut/Mut}$ mouse; M. Fischer and M. Jaritz performed the bioinformatic analysis of all RNA-seq and ChIP-seq data, respectively; M. Wöhner, H. Tagoh, and M. Busslinger planned the project, designed the experiments, and wrote the manuscript.

Submitted: 23 December 2015
Accepted: 4 May 2016

REFERENCES

Anders, S., P.T. Pyl, and W. Huber. 2015. HTSeq--a Python framework to work with high-throughput sequencing data. *Bioinformatics.* 31:166–169. http://dx.doi.org/10.1093/bioinformatics/btu638

Aszódi, A. 2012. MULTOVL: fast multiple overlaps of genomic regions. *Bioinformatics.* 28:3318–3319. http://dx.doi.org/10.1093/bioinformatics/bts607

Bain, G., S. Gruenwald, and C. Murre. 1993. E2A and E2-2 are subunits of B-cell-specific E2-box DNA-binding proteins. *Mol. Cell. Biol.* 13:3522–3529. http://dx.doi.org/10.1128/MCB.13.6.3522

Bain, G., E.C.R. Maandag, D.J. Izon, D. Amsen, A.M. Kruisbeek, B.C. Weintraub, I. Krop, M.S. Schlissel, A.J. Feeney, M. van Roon, et al. 1994. E2A proteins are required for proper B cell development and initiation of immunoglobulin gene rearrangements. *Cell.* 79:885–892. http://dx.doi.org/10.1016/0092-8674(94)90077-9

Bayly, R., L. Chuen, R.A. Currie, B.D. Hyndman, R. Casselman, G.A. Blobel, and D.P. LeBrun. 2004. E2A-PBX1 interacts directly with the KIX domain of CBP/p300 in the induction of proliferation in primary hematopoietic cells. *J. Biol. Chem.* 279:55362–55371. http://dx.doi.org/10.1074/jbc.M408654200

Bergqvist, I., M. Eriksson, J. Saarikettu, B. Eriksson, B. Corneliussen, T. Grundström, and D. Holmberg. 2000. The basic helix-loop-helix transcription factor E2-2 is involved in T lymphocyte development. *Eur. J. Immunol.* 30:2857–2863. http://dx.doi.org/10.1002/1521-4141(200010)30:10<2857::AID-IMMU2857>3.0.CO;2-G

Bradney, C., M. Hjelmeland, Y. Komatsu, M. Yoshida, T.P. Yao, and Y. Zhuang. 2003. Regulation of E2A activities by histone acetyltransferases in B lymphocyte development. *J. Biol. Chem.* 278:2370–2376. http://dx.doi.org/10.1074/jbc.M211464200

Buenrostro, J.D., P.G. Giresi, L.C. Zaba, H.Y. Chang, and W.J. Greenleaf. 2013. Transposition of native chromatin for fast and sensitive epigenomic profiling of open chromatin, DNA-binding proteins and nucleosome position. *Nat. Methods.* 10:1213–1218. http://dx.doi.org/10.1038/nmeth.2688

Chaudhuri, J., and F.W. Alt. 2004. Class-switch recombination: interplay of transcription, DNA deamination and DNA repair. *Nat. Rev. Immunol.* 4:541–552. http://dx.doi.org/10.1038/nri1395

Chen, W.-Y., J. Zhang, H. Geng, Z. Du, T. Nakadai, and R.G. Roeder. 2013. A TAF4 coactivator function for E proteins that involves enhanced TFIID binding. *Genes Dev.* 27:1596–1609. http://dx.doi.org/10.1101/gad.216192.113

Crouch, E.E., Z. Li, M. Takizawa, S. Fichtner-Feigl, P. Gourzi, C. Montaño, L. Feigenbaum, P. Wilson, S. Janz, F.N. Papavasiliou, and R. Casellas. 2007. Regulation of AID expression in the immune response. *J. Exp. Med.* 204:1145–1156. http://dx.doi.org/10.1084/jem.20061952

Cunningham, F., M.R. Amode, D. Barrell, K. Beal, K. Billis, S. Brent, D. Carvalho-Silva, P. Clapham, G. Coates, S. Fitzgerald, et al. 2015. Ensembl 2015. *Nucleic Acids Res.* 43(D1):D662–D669. http://dx.doi.org/10.1093/nar/gku1010

Delogu, A., A. Schebesta, Q. Sun, K. Aschenbrenner, T. Perlot, and M. Busslinger. 2006. Gene repression by Pax5 in B cells is essential for blood cell homeostasis and is reversed in plasma cells. *Immunity.* 24:269–281. http://dx.doi.org/10.1016/j.immuni.2006.01.012

Hagège, H., P. Klous, C. Braem, E. Splinter, J. Dekker, G. Cathala, W. de Laat, and T. Forné. 2007. Quantitative analysis of chromosome conformation capture assays (3C-qPCR). *Nat. Protoc.* 2:1722–1733. http://dx.doi.org/10.1038/nprot.2007.243

Heavey, B., C. Charalambous, C. Cobaleda, and M. Busslinger. 2003. Myeloid lineage switch of Pax5 mutant but not wild-type B cell progenitors by C/EBPalpha and GATA factors. *EMBO J.* 22:3887–3897. http://dx.doi.org/10.1093/emboj/cdg380

Huong, T., M. Kobayashi, M. Nakata, G. Shioi, H. Miyachi, T. Honjo, and H. Nagaoka. 2013. *In vivo* analysis of *Aicda* gene regulation: a critical balance between upstream enhancers and intronic silencers governs appropriate expression. *PLoS One.* 8:e61433. http://dx.doi.org/10.1371/journal.pone.0061433

Inlay, M.A., H. Tian, T. Lin, and Y. Xu. 2004. Important roles for E protein binding sites within the immunoglobulin κ chain intronic enhancer in activating Vkappa Jkappa rearrangement. *J. Exp. Med.* 200:1205–1211. http://dx.doi.org/10.1084/jem.20041135

Jones-Mason, M.E., X. Zhao, D. Kappes, A. Lasorella, A. Iavarone, and Y. Zhuang. 2012. E protein transcription factors are required for the development of CD4$^+$ lineage T cells. *Immunity.* 36:348–361. http://dx.doi.org/10.1016/j.immuni.2012.02.010

Kallies, A., J. Hasbold, D.M. Tarlinton, W. Dietrich, L.M. Corcoran, P.D. Hodgkin, and S.L. Nutt. 2004. Plasma cell ontogeny defined by quantitative changes in blimp-1 expression. *J. Exp. Med.* 200:967–977. http://dx.doi.org/10.1084/jem.20040973

Kallies, A., J. Hasbold, K. Fairfax, C. Pridans, D. Emslie, B.S. McKenzie, A.M. Lew, L.M. Corcoran, P.D. Hodgkin, D.M. Tarlinton, and S.L. Nutt. 2007. Initiation of plasma-cell differentiation is independent of the transcription factor Blimp-1. *Immunity.* 26:555–566. http://dx.doi.org/10.1016/j.immuni.2007.04.007

Kee, B.L. 2009. E and ID proteins branch out. *Nat. Rev. Immunol.* 9:175–184. http://dx.doi.org/10.1038/nri2507

Kieffer-Kwon, K.R., Z. Tang, E. Mathe, J. Qian, M.H. Sung, G. Li, W. Resch, S. Baek, N. Pruett, L. Grøntved, et al. 2013. Interactome maps of mouse gene regulatory domains reveal basic principles of transcriptional regulation. *Cell.* 155:1507–1520. http://dx.doi.org/10.1016/j.cell.2013.11.039

Kohwi-Shigematsu, T., Y. Kohwi, K. Takahashi, H.W. Richards, S.D. Ayers, H.-J. Han, and S. Cai. 2012. SATB1-mediated functional packaging of chromatin into loops. *Methods.* 58:243–254. http://dx.doi.org/10.1016/j.ymeth.2012.06.019

Kwon, K., C. Hutter, Q. Sun, I. Bilic, C. Cobaleda, S. Malin, and M. Busslinger. 2008. Instructive role of the transcription factor E2A in early B lymphopoiesis and germinal center B cell development. *Immunity.* 28:751–762. http://dx.doi.org/10.1016/j.immuni.2008.04.014

Love, M.I., W. Huber, and S. Anders. 2014. Moderated estimation of fold change and dispersion for RNA-seq data with DESeq2. *Genome Biol.* 15:550. http://dx.doi.org/10.1186/s13059-014-0550-8

Machanick, P., and T.L. Bailey. 2011. MEME-ChIP: motif analysis of large DNA datasets. *Bioinformatics.* 27:1696–1697. http://dx.doi.org/10.1093/bioinformatics/btr189

Martins, G., and K. Calame. 2008. Regulation and functions of Blimp-1 in T and B lymphocytes. *Annu. Rev. Immunol.* 26:133–169. http://dx.doi.org/10.1146/annurev.immunol.26.021607.090241

Medvedovic, J., A. Ebert, H. Tagoh, I.M. Tamir, T.A. Schwickert, M. Novatchkova, Q. Sun, P.J. Huis In 't Veld, C. Guo, H.S. Yoon, et al. 2013. Flexible long-range loops in the V_H gene region of the *Igh* locus facilitate the generation of a diverse antibody repertoire. *Immunity.* 39:229–244. http://dx.doi.org/10.1016/j.immuni.2013.08.011

Minnich, M., H. Tagoh, P. Bönelt, E. Axelsson, M. Fischer, B. Cebolla, A. Tarakhovsky, S.L. Nutt, M. Jaritz, and M. Busslinger. 2016. Multifunctional role of the transcription factor Blimp-1 in coordinating plasma cell differentiation. *Nat. Immunol.* 17:331–343. http://dx.doi.org/10.1038/ni.3349

Muramatsu, M., K. Kinoshita, S. Fagarasan, S. Yamada, Y. Shinkai, and T. Honjo. 2000. Class switch recombination and hypermutation require activation-induced cytidine deaminase (AID), a potential RNA editing enzyme. *Cell.* 102:553–563. http://dx.doi.org/10.1016/S0092-8674(00)00078-7

Murre, C. 2005. Helix-loop-helix proteins and lymphocyte development. *Nat. Immunol.* 6:1079–1086. http://dx.doi.org/10.1038/ni1260

Murre, C., P.S. McCaw, and D. Baltimore. 1989. A new DNA binding and dimerization motif in immunoglobulin enhancer binding, *daughterless, MyoD*, and *myc* proteins. *Cell.* 56:777–783. http://dx.doi.org/10.1016/0092-8674(89)90682-X

Nojima, T., K. Haniuda, T. Moutai, M. Matsudaira, S. Mizokawa, I. Shiratori, T. Azuma, and D. Kitamura. 2011. *In-vitro* derived germinal centre B cells differentially generate memory B or plasma cells *in vivo*. *Nat. Commun.* 2:465. http://dx.doi.org/10.1038/ncomms1475

Nurieva, R.I., Y. Chung, D. Hwang, X.O. Yang, H.S. Kang, L. Ma, Y.H. Wang, S.S. Watowich, A.M. Jetten, Q. Tian, and C. Dong. 2008. Generation of T follicular helper cells is mediated by interleukin-21 but independent of T helper 1, 2, or 17 cell lineages. *Immunity.* 29:138–149. http://dx.doi.org/10.1016/j.immuni.2008.05.009

Nutt, S.L., P.D. Hodgkin, D.M. Tarlinton, and L.M. Corcoran. 2015. The generation of antibody-secreting plasma cells. *Nat. Rev. Immunol.* 15:160–171. http://dx.doi.org/10.1038/nri3795

Ohinata, Y., B. Payer, D. O'Carroll, K. Ancelin, Y. Ono, M. Sano, S.C. Barton, T. Obukhanych, M. Nussenzweig, A. Tarakhovsky, et al. 2005. Blimp1 is a critical determinant of the germ cell lineage in mice. *Nature.* 436:207–213. http://dx.doi.org/10.1038/nature03813

Qin, X.-F., A. Reichlin, Y. Luo, R.G. Roeder, and M.C. Nussenzweig. 1998. OCA-B integrates B cell antigen receptor-, CD40L- and IL 4-mediated signals for the germinal center pathway of B cell development. *EMBO J.* 17:5066–5075. http://dx.doi.org/10.1093/emboj/17.17.5066

Quong, M.W., D.P. Harris, S.L. Swain, and C. Murre. 1999. E2A activity is induced during B-cell activation to promote immunoglobulin class switch recombination. *EMBO J.* 18:6307–6318. http://dx.doi.org/10.1093/emboj/18.22.6307

Reimold, A.M., N.N. Iwakoshi, J. Manis, P. Vallabhajosyula, E. Szomolanyi-Tsuda, E.M. Gravallese, D. Friend, M.J. Grusby, F. Alt, and L.H. Glimcher. 2001. Plasma cell differentiation requires the transcription factor XBP-1. *Nature.* 412:300–307. http://dx.doi.org/10.1038/35085509

Revilla-i-Domingo, R., I. Bilic, B. Vilagos, H. Tagoh, A. Ebert, I.M. Tamir, L. Smeenk, J. Trupke, A. Sommer, M. Jaritz, and M. Busslinger. 2012. The B-cell identity factor Pax5 regulates distinct transcriptional programmes in early and late B lymphopoiesis. *EMBO J.* 31:3130–3146. http://dx.doi.org/10.1038/emboj.2012.155

Saintamand, A., P. Rouaud, F. Saad, G. Rios, M. Cogné, and Y. Denizot. 2015. Elucidation of *IgH* 3′ region regulatory role during class switch recombination via germline deletion. *Nat. Commun.* 6:7084. http://dx.doi.org/10.1038/ncomms8084

Sayegh, C.E., M.W. Quong, Y. Agata, and C. Murre. 2003. E-proteins directly regulate expression of activation-induced deaminase in mature B cells. *Nat. Immunol.* 4:586–593. http://dx.doi.org/10.1038/ni923

Schebesta, A., S. McManus, G. Salvagiotto, A. Delogu, G.A. Busslinger, and M. Busslinger. 2007. Transcription factor Pax5 activates the chromatin of key genes involved in B cell signaling, adhesion, migration, and immune function. *Immunity.* 27:49–63. http://dx.doi.org/10.1016/j.immuni.2007.05.019

Schubart, D.B., A. Rolink, M.H. Kosco-Vilbois, F. Botteri, and P. Matthias. 1996. B-cell-specific coactivator OBF-1/OCA-B/Bob1 required for immune response and germinal centre formation. *Nature.* 383:538–542. http://dx.doi.org/10.1038/383538a0

Shapiro-Shelef, M., K.-I. Lin, L.J. McHeyzer-Williams, J. Liao, M.G. McHeyzer-Williams, and K. Calame. 2003. Blimp-1 is required for the formation of immunoglobulin secreting plasma cells and pre-plasma memory B cells. *Immunity.* 19:607–620. http://dx.doi.org/10.1016/S1074-7613(03)00267-X

Shen, C.-P., and T. Kadesch. 1995. B-cell-specific DNA binding by an E47 homodimer. *Mol. Cell. Biol.* 15:4518–4524. http://dx.doi.org/10.1128/MCB.15.8.4518

Smith, K.G., A. Light, G.J. Nossal, and D.M. Tarlinton. 1997. The extent of affinity maturation differs between the memory and antibody-forming cell compartments in the primary immune response. *EMBO J.* 16:2996–3006. http://dx.doi.org/10.1093/emboj/16.11.2996

Splinter, E., H. Heath, J. Kooren, R.-J. Palstra, P. Klous, F. Grosveld, N. Galjart, and W. de Laat. 2006. CTCF mediates long-range chromatin looping and local histone modification in the β-globin locus. *Genes Dev.* 20:2349–2354. http://dx.doi.org/10.1101/gad.399506

Taubenheim, N., D.M. Tarlinton, S. Crawford, L.M. Corcoran, P.D. Hodgkin, and S.L. Nutt. 2012. High rate of antibody secretion is not integral to plasma cell differentiation as revealed by XBP-1 deficiency. *J. Immunol.* 189:3328–3338. http://dx.doi.org/10.4049/jimmunol.1201042

Trapnell, C., L. Pachter, and S.L. Salzberg. 2009. TopHat: discovering splice junctions with RNA-Seq. *Bioinformatics.* 25:1105–1111. http://dx.doi.org/10.1093/bioinformatics/btp120

Victora, G.D., and M.C. Nussenzweig. 2012. Germinal centers. *Annu. Rev. Immunol.* 30:429–457. http://dx.doi.org/10.1146/annurev-immunol-020711-075032

Vincent-Fabert, C., R. Fiancette, E. Pinaud, V. Truffinet, N. Cogné, M. Cogné, and Y. Denizot. 2010. Genomic deletion of the whole IgH 3′ regulatory region (hs3a, hs1,2, hs3b, and hs4) dramatically affects class switch recombination and Ig secretion to all isotypes. *Blood.* 116:1895–1898. http://dx.doi.org/10.1182/blood-2010-01-264689

Yang, H., H. Wang, C.S. Shivalila, A.W. Cheng, L. Shi, and R. Jaenisch. 2013. One-step generation of mice carrying reporter and conditional alleles

by CRISPR/Cas-mediated genome engineering. *Cell*. 154:1370–1379. http://dx.doi.org/10.1016/j.cell.2013.08.022

Ying, C.Y., D. Dominguez-Sola, M. Fabi, I.C. Lorenz, S. Hussein, M. Bansal, A. Califano, L. Pasqualucci, K. Basso, and R. Dalla-Favera. 2013. MEF2B mutations lead to deregulated expression of the oncogene *BCL6* in diffuse large B cell lymphoma. *Nat. Immunol.* 14:1084–1092. http://dx.doi.org/10.1038/ni.2688

Zhang, Y., T. Liu, C.A. Meyer, J. Eeckhoute, D.S. Johnson, B.E. Bernstein, C. Nusbaum, R.M. Myers, M. Brown, W. Li, and X.S. Liu. 2008. Model-based analysis of ChIP-Seq (MACS). *Genome Biol.* 9:R137. http://dx.doi.org/10.1186/gb-2008-9-9-r137

Zhuang, Y., P. Soriano, and H. Weintraub. 1994. The helix-loop-helix gene E2A is required for B cell formation. *Cell*. 79:875–884. http://dx.doi.org/10.1016/0092-8674(94)90076-0